Author Manuscript

Author Manuscript

Author Manuscript

Author Manuscript

HHS Public Access

Author manuscript

J Immunol. Author manuscript; available in PMC 2016 April 15.

Published in final edited form as:

J Immunol. 2015 April 15; 194(8): 3697–3712. doi:10.4049/jimmunol.1402785.

Regulation of Pulmonary Graft-versus-Host Disease by IL-26^{+}CD26^{+}CD4 T Lymphocytes

Kei Ohnuma[*], **Ryo Hatano**[*], **Thomas M. Aune**[†], **Haruna Otsuka**[*], **Satoshi Iwata**[*], **Nam H. Dang**[‡], **Taketo Yamada**[§], and **Chikao Morimoto**[*]

[*]Department of Therapy Development and Innovation for Immune Disorders and Cancers, Graduate School of Medicine, Juntendo University, Tokyo 113-8421, Japan

[†]Department of Medicine, Vanderbilt University School of Medicine, Vanderbilt University Medical Center, Nashville, TN 37232

[‡]Division of Hematology and Oncology, University of Florida, Gainesville, FL 32610

[§]Department of Pathology, Keio University School of Medicine, Tokyo, 160-8582, Japan

Abstract

Obliterative bronchiolitis is a potentially life-threatening noninfectious pulmonary complication after allogeneic hematopoietic stem cell transplantation and the only pathognomonic manifestation of pulmonary chronic graft-versus-host disease (cGVHD). In the current study, we identified a novel effect of IL-26 on transplant-related obliterative bronchiolitis. Sublethally irradiated NOD/Shi-*scid*IL2rγ^{null} mice transplanted with human umbilical cord blood (HuCB mice) gradually developed clinical signs of graft-versus-host disease (GVHD) such as loss of weight, ruffled fur, and alopecia. Histologically, lung of HuCB mice exhibited obliterative bronchiolitis with increased collagen deposition and predominant infiltration with human IL-26^{+}CD26^{+}CD4 T cells. Concomitantly, skin manifested fat loss and sclerosis of the reticular dermis in the presence of apoptosis of the basilar keratinocytes, whereas the liver exhibited portal fibrosis and cholestasis. Moreover, although IL-26 is absent from rodents, we showed that IL-26 increased collagen synthesis in fibroblasts and promoted lung fibrosis in a murine GVHD model using *IL-26* transgenic mice. In vitro analysis demonstrated a significant increase in IL-26 production by HuCB CD4 T cells following CD26 costimulation, whereas Ig Fc domain fused with the N-terminal of caveolin-1 (Cav-Ig), the ligand for CD26, effectively inhibited production of IL-26. Administration of Cav-Ig before or after onset of GVHD impeded the development of clinical and histologic features of GVHD without interrupting engraftment of donor-derived human cells, with preservation of the graft-versus-leukemia effect. These results therefore provide proof of principle that cGVHD of the lungs is caused in part by IL-26^{+}CD26^{+}CD4 T cells, and that treatment with Cav-Ig could be beneficial for cGVHD prevention and therapy.

Address correspondence and reprint requests to Prof. Chikao Morimoto, Department of Therapy Development and Innovation for Immune Disorders and Cancers, Graduate School of Medicine, Juntendo University, 2-1-1, Hongo, Bunkyo-ku, Tokyo 113-8421, Japan. morimoto@ims.u-tokyo.ac.jp.

Disclosures

The authors have no financial conflicts of interest.

The online version of this article contains supplemental material.

Author Manuscript Author Manuscript Author Manuscript Author Manuscript

Allogeneic hematopoietic stem cell transplantation (alloHSCT) is a potentially curative treatment for many diseases arising from hematopoietic cells (1). However, chronic graft-versus-host disease (cGVHD) remains a significant barrier to successful alloHSCT (2). In particular, the lung damage in cGVHD causes potentially life-threatening complications (3). According to the National Institutes of Health consensus criteria, obliterative bronchiolitis (historically named bronchiolitis obliterans by pathologists) is the only pathognomonic manifestation of pulmonary cGVHD (4). It is recognized that obliterative bronchiolitis has been associated with an increased risk of death, and patients diagnosed with obliterative bronchiolitis after alloHSCT have a 5-y survival rate of only 10% (5).

Although many preclinical models mimicking human cGVHD including obliterative bronchiolitis have been established (6), control of obliterative bronchiolitis after alloHSCT has not yet been achieved thoroughly (7). The clinical application of murine data is limited because multiple, yet limited schema have arisen to identify alloimmune reactions in cross-species comparisons. For instance, one extensively used model of cGVHD clearly exhibited immune-complex glomerulonephritis, which is rarely seen in human cGVHD (8). Moreover, transfer of autoantibodies from mice with GVHD to normal mice failed to cause autoimmune pathology (9). These limitations are based on preparative regimens, composition of donor graft, and genetic backgrounds of donor and recipient animals (6). In addition, recent work has demonstrated multiple differences in immunological functions between humans and mice (10, 11). In contrast, because in vivo T cell depletion is the only prophylactic measure that effectively decreases the incidence of cGVHD (2, 12), donor T cells clearly play an important role in the immune pathology of cGVHD. Taken together, to develop novel therapeutic strategies for use in the clinical setting, the establishment of a humanized murine model of cGVHD is urgently needed. We previously analyzed a humanized murine acute GVHD (aGVHD) model involving mice transplanted with human adult PBL, and showed that liver and skin were predominantly involved as target organs in this model of aGVHD, which was clearly impeded by the administration of anti-CD26 mAb (13). Our data suggest that $CD26^+$ T cells play an effector role in this aGVHD model. However, because the mice studied in our previous work succumbed to aGVHD ~4 wk after transplantation of human adult PBL, this early-onset model of aGVHD does not permit the assessment of longer-term consequences of interventional therapies such as the development of obliterative bronchiolitis, a form of cGVHD of the lung.

CD26 is associated with T cell signal transduction processes as a costimulatory molecule, as well as being a marker of T cell activation in human adult PBL (14–16). In fact, patients with autoimmune diseases such as multiple sclerosis and rheumatoid arthritis (RA) have been found to have increased numbers of $CD26^+$CD4 T cells in both inflamed tissues and the peripheral blood, with enhancement of CD26 expression in these autoimmune diseases correlating with disease severity (17). Previously, we have demonstrated that caveolin-1 is a costimulatory ligand for human CD26, and that CD26 on activated memory T cells interacts with caveolin-1 on recall Ag-primed monocytes (18, 19). More recently, we demonstrated in in vitro experiments that blockade of CD26-mediated T cell costimulation by soluble Fc fusion proteins containing the N-terminal domain of caveolin-1 (Cav-Ig) diminished primary and secondary proliferative responses not only to recall Ag, but also to unrelated allogeneic

Author Manuscript Author Manuscript Author Manuscript Author Manuscript

APC (20). In contrast to adult PBL, the human umbilical cord blood (HuCB) lymphocytes have been reported to be immature, predominantly consisting of $CD45RA^+$ naive cells (21, 22). We previously showed that, although all HuCB CD4 T cells constitutively expressed CD26, CD26-mediated costimulation was considerably attenuated in HuCB CD4 T cells, compared with the robust activation via CD26 costimulation of adult PBL (21). Additionally, HuCB CD4 T cells exhibited only slight activation after long-sustained stimulation of CD26. These findings provided further insights into the cellular mechanisms of immature immune response in HuCB. Furthermore, it has been reported that humanized mice transplanted with human hematopoietic stem cell (HSC) isolated from HuCB exhibited human hematopoiesis reconstitution as well as B cell engraftment with a similar Ab repertoire as observed in B cells in human (23, 24). Based on these findings, we hypothesized that HuCB naive CD4 T cells gradually acquire a xenogeneic response via attenuated stimulatory signaling with indolent inflammation in the target organs, leading eventually to chronic inflammatory changes. We therefore sought to develop a humanized murine pulmonary cGVHD model utilizing HuCB donor cells, and to overcome the limitations seen in the humanized murine aGVHD model such as vigorous activation of all engrafted T cells and extensive loss of B cell maturation and activation (23).

In the current study, we established a xenogeneic pulmonary cGVHD murine model induced by transplantation of HuCB, which exhibited obliterative bronchiolitis as well as sclerodermatous skin and primary biliary cirrhosis-like liver. Moreover, we determined a novel effect of IL-26 produced by donor-derived human CD4 T cells on fibroproliferation of obliterative bronchiolitis, which was also shown in the murine alloHSCT model using human *IL26* transgenic mice. In addition, our findings indicated a decrease of collagen deposition in the lung of xenogeneic pulmonary cGVHD mice treated with anti–IL-26 neutralizing Ab. Our analysis of a patient specimen demonstrated the predominant infiltration of $IL\text{-}26^+CD26^+$CD4 T cells in the lung of obliterative bronchiolitis after alloHSCT. In in vitro experiments, we showed that IL-26 of HuCB CD4 T cells was produced via CD26 costimulation by its ligand caveolin-1, whereas CD28 costimulation did not generally enhance IL-26 production. Furthermore, abrogation of CD26 costimulation by Cav-Ig before or during early onset of GVHD impeded the development of pulmonary cGVHD. These results provide proof of principle that human $IL\text{-}26^+CD26^+$CD4 T cells are involved in the pathophysiology of pulmonary cGVHD, and that blockade of CD26 costimulation by Cav-Ig appears to be a promising novel therapeutic strategy for the clinical control of cGVHD.

Materials and Methods

Abs, reagents, and cells

Mouse mAbs to human CD3 (OKT3, IgG2b), CD26 (1F7, IgG1), and CD28 (4B10, IgG1) for costimulation experiments were developed in our laboratory (25). Anti–IL-26 goat polyclonal Ab (pAb) (AF1375), which is available for neutralizing experiments (26), was obtained from R&D Systems (Minneapolis, MN). Human rIL-26 was purchased from R&D Systems and stocked at 1 μg ml^{-1} in PBS. Cav-Ig and its control Fc protein were made in our laboratory, with previous references in the literature (27). Normal human lung fibroblast

Author Manuscript Author Manuscript Author Manuscript Author Manuscript

(NHLF) and the culture medium FGF-2 were purchased from LONZA (Walkersville, MD). Mouse fibroblast cell line NIH3T3 and mononuclear cells (MNCs) isolated from HuCB with Ficoll density gradation method were purchased from RIKEN BioResource Center (Tsukuba, Japan). T cell–depleted $CD34^+$ cells were purified from MNCs of HuCB using human CD34 MicroBead Kit (Miltenyi Biotec, Bergisch Gladbach, Germany).

Mice

NOD/SCID/$\gamma_c^{-/-}$ NOD.Cg-Prkdcscid Il2rgtm1Sug/Jic mice (NOG mice) (H-2^d) were purchased from the Central Institute for Experimental Animals (Kawasaki, Japan). C57BL/6 (B6) mice (H-2^b) were obtained from CLEA Japan (Tokyo, Japan). B6 mice carrying a 190-kb bacterial artificial chromosome (BAC) transgene with human *IFNG* and *IL26* gene (190-*IFNG* transgenic [Tg]) and a BAC Tg-deleting conserved noncoding sequence (CNS) positioned upstream of the *IFNG* transcription start site (ΔCNS-77 Tg) were developed in Thomas Aune's laboratory (28). All mice were housed in a specific pathogen-free facility in microisolator cages. Mice were used at 8–12 wk. Animal protocol was approved by the Institutional Animal Care and Use Committee.

Transplantation and assessment of GVHD

On day −1, NOG mice received 200 cGy irradiation. On day 0, mice were injected i.p. with 1×10^7 MNC (whole CB transplant) or 1×10^5 $CD34^+$ cells ($CD34^+$ transplant) purified from HuCB. Mice were assessed for survival daily and weighed thrice weekly. In IL-26 blockade experiments, mice were treated with anti–IL-26 pAb or control goat IgG at 50 μg per dose i.p. thrice per week from day +21 until day +32 (total six doses). In cGVHD prevention experiments, mice were given human Cav-Ig, or control human Fc at 100 μg per dose i.p. thrice per week from day +1 until day +28 (total 12 doses). In cGVHD treatment experiments, at onset of first clinical signs of disease 28 d after HuCB transplantation, mice were given human Cav-Ig, or control human Fc at 100 μg per dose i.p. thrice per week from day +29 until day +56 (total 12 doses) after confirmation of engraftment. Engraftment of HuCB was confirmed by quantification of human $CD45^+$ leukocytes in mouse peripheral blood using flow cytometry. The clinical GVHD score was assessed at least weekly according to the previous reference in the literature (29). For allogeneic bone marrow transplantation experiments using Tg mice, sublethally irradiated (200 cGy) NOG mice were transplanted with 1×10^7 bone marrow and 1×10^6 splenocytes isolated from 190-*IFNG* Tg, ΔCNS-77 Tg or parental B6 (B6 wild-type) mice. Recipients were sacrificed at 4 wk posttransplantation, and the lungs were removed for histopathological evaluation.

Tissue histopathology and immunohistochemistry

Skin from the upper back, the left lung, and liver specimens of recipients were fixed in 10% formalin, embedded in paraffin, sectioned, mounted in slides, and stained with H&E to determine pathology. The lung specimen of a patient undergoing an allogeneic peripheral blood-stem cell transplant (alloPBSCT) for acute lymphoblastic leukemia (ALL) was prepared for histopathologic and immunohistochemical studies by the same method as described above. Images were captured with an Olympus digital camera DP21 attached to an Olympus BX43 microscope using CellSens software (OLYMPUS, Tokyo, Japan). Slides

Author Manuscript Author Manuscript Author Manuscript Author Manuscript

were scored by a pathologist blinded to experimental groups. The GVHD pathology score was assessed according to the previous references in the literature (29–31). For detection of collagen, slides were stained with Azan-Mallory staining. Abs used in immunohistochemistry were anti-human CD4 mAb (4B12, mouse IgG1) and anti-human CD8 mAb (C8/144B, mouse IgG1) from Dako (Tokyo, Japan), anti-human CD26 goat pAb (AF1180) from R&D Systems, anti–IL-26 rabbit pAb (bs-2626R) from Bioss (Wobum, MA), and anti–IL-17A rabbit pAb (H-132) from Santa Cruz Biotechnology (Santa Cruz, CA). Immunohistochemical staining for CD4, CD8, CD26, or IL-26 was performed at the Department of Pathology, Keio University School of Medicine (Tokyo, Japan), as described previously (32). Immunohistochemical staining for IL-17A was conducted at the laboratory of MorphoTechnology (Sapporo, Japan).

Real-time quantitative RT-PCR

In experiments assessing expression of mRNA of effector molecules, a single-cell suspension was isolated from the lung of recipient mice using Lung Dissociation Kit (Miltenyi Biotec), followed by purification of human CD4 T cells using human CD4 MicroBeads (Miltenyi Biotec). Isolation and quantification of mRNA were performed, as described previously (33). Expression levels of mRNA were calculated on the basis of standard curves generated for each gene, and hypoxanthine phosphoribosyltransferase 1 (HPRT1) mRNA was used as an invariant control. Sequences of primers used in real-time RT-PCR analysis are as follows: human IL-2, forward 5′-AGAAGGCCACAGAACTGAAAC-3′, reverse 5′-GCTGTCTCATCAGCATATTCAC-3′; human IL-4, forward 5′-CAGTTCTACAGCCACCATGAGA-3′, reverse 5′-CGTCTTTAGCCTTTCCAAGAAG-3′; human IL-6, forward 5′-GCCAGAGCTGTGCAGATGAG-3′, reverse 5′-TCAGCAGGCTGGCATTTG-3′; human IL-10, forward 5′-CTGGGGGAGAACCTGAAGAC-3′, reverse 5′-TGGCTTTGTAGATGCCTTTCTC-3′; human IL-17A, forward 5′-ACATCCATAACCGGAATACCAA-3′, reverse 5′-ACATCCATAACCGGAATACCAA-3′; human IL-21, forward 5′-GACACTGGTCCACAAATCAAGCTC-3′, reverse 5′-TGCTGACTTTAGTTGGGCCTTC-3′; human IL-26, forward 5′-CAATTGCAAGGCTGCAAGAA-3′, reverse 5′-TCTCTAGCTGATGAAGCACAGGAA-3′; human IFN-γ, forward 5′-GTGTGGAGACCATCAAGGAAG-3′, reverse 5′-ATGTATTGCTTTGCGTTGGA-3′; human TNF-α, forward 5′-TCAGCCTCTTCTCCTTCCTG-3′, reverse 5′-TTTGCTACAACATGGGCTACA-3′; human CD26, forward 5′-GTACACAGAACGTTACATGGGTCTC-3′, reverse 5′-TCAGCTCTGCTCATGACTGTTG-3′; and human HPRT1, forward 5′-CAGTCAACAGGGGACATAAAAG-3′, reverse 5′-CCTGACCAAGGAAAGCAAAG-3′.

Flow cytometry

The following Abs were from BD Biosciences (San Jose, CA): anti-human CD3 (UCHT1, mouse IgG1), anti-human CD4 (RPA-Ta, mouse IgG1), antihuman CD8 (HIT8a, mouse IgG1), anti-human CD14 (M5E2, mouse IgG1), anti-human CD19 (HIB19, mouse IgG1), anti-human CD26 (M-A261, mouse IgG1), anti-human CD45 (HI30, mouse IgG1), anti-

Author Manuscript Author Manuscript Author Manuscript Author Manuscript

human CD56 (B159, mouse IgG1), anti-human IFN-γ (B27, mouse IgG1), anti-human IL-17A (N49-653, mouse IgG1) mAbs, and relevant control mAbs of the same Ig isotype. Fluorescent conjugates were FITC, PE, PerCP-Cy5.5, and allophycocyanin. Anti–IL-10RB rabbit pAb (bs-2602R) was purchased from Bioss, and anti–IL-20RA rabbit pAb (06–1073) from Millipore (Billerica, MA). Anti–IL-10RB and anti–IL-20RA pAbs recognize both human and murine Ags. mAb staining of intracellular IL-26 (clone 510414, mouse IgG1) was purchased from R&D Systems, being conjugated with Alexa Fluor 647 using Antibody Labeling Kit (Invitrogen, Carlsbad, CA). RBCs in samples of murine peripheral blood were lysed using BD FACS Lysing Solution (BD Biosciences). For analyzing lymphocytes infiltrated in the lung, a single-cell suspension was prepared using Lung Dissociation Kit, followed by purification with human CD45 MicroBeads (Miltenyi Biotec). For intracellular cytokine analysis, purified human $CD45^+$ cells were restimulated for 4 h with 25 ng ml^{-1} PMA (Sigma-Aldrich, St. Louis, MO) plus 1 μg ml^{-1} ionomycin (Sigma-Aldrich) in the presence of BD GolgiPlug (BD Biosciences). Intracellular flow cytometry was performed according to the manufacturer's instructions using Human Intracellular Cytokine Staining Kit (BD Biosciences). Analysis was performed on two-laser FACSCalibur (BD Biosciences), and files were analyzed in CellQuest software (BD Biosciences).

Western blotting

To analyze expression of IL-20RA or IL-10RB, 10 μg lysates of NHLF and NIH3T3 were prepared using radioimmunoprecipitation assay (RIPA) buffer, being resolved by SDS-PAGE in reducing condition and immunoblotted using anti–IL-20RA (ab25922; Abcam, Cambridge, MA) or anti–IL-10RB (bs-2602R; Bioss) rabbit pAbs recognizing both human and murine Ags. For analysis of phosphorylated STAT3 induced by exogenous IL-26, 1×10^5 cells were seeded in 96-well flat-bottom plate, and the next day IL-26 (10 ng ml^{-1} in PBS) was added to each well. Cells were harvested at each time point, and cell lysates were prepared in RIPA buffer containing Halt Protease and Phosphatase inhibitor mixture (Thermo Fisher Scientific, Waltham, MA). Each 10 μg lysate was resolved by SDS-PAGE in reducing condition and immunoblotted with antiphosphorylated STAT3 (pY-STAT3) (#11045; SAB, Collage Park, MD) recognizing both human and murine Ags, followed by stripping and reprobing with anti-STAT3 pAb (total STAT3) (GTX15523; GeneTex, Irvine, CA) recognizing both human and murine Ags.

Measurement of cytokines and soluble CD26/dipeptidyl peptidase IV

The collected sera were analyzed for inflammatory cytokines other than human IL-26 using Bio-Plex Pro Human Cytokine Assay (Bio-Rad Laboratories, Hercules, CA). IL-26 was assayed using Human IL-26 ELISA Kit (CUSABIO, Hubei, China). Assay for soluble CD26/dipeptidyl peptidase IV (DPP4) was developed in our laboratory (34). All samples were run in triplicates.

In vitro and in vivo collagen assay

NHLF or NIH3T3 cells were seeded in 96-well flat-bottom plate (1×10^5/well), and the next day IL-26 (0.1, 2.0, 5.0, or 10 ng ml^{-1} in PBS) or PBS alone was added to each well. In neutralizing experiments, neutralizing anti–IL-20RA rabbit pAb (06-1073; R&D Systems) or control rabbit Ig (10 μg ml^{-1} each) was added to each well 1 h before exogenous IL-26

Author Manuscript Author Manuscript Author Manuscript Author Manuscript

was added. The supernatants were harvested 48 h after IL-26 was added, followed by measuring soluble collagen using Sircol Collagen Assay Kit (Biocolor, County Antrim, U.K.). The total collagen of the left lung was extracted using acid–pepsin solution and measured according to the manufacturer's instructions of Sircol Collagen Assay Kit. All samples were examined in triplicates.

In vitro costimulation assay

For analysis of mRNA expression, CD4 T cells were purified isolated from HuCB MNCs, and 1×10^5 cells/well were seeded in 96-well flat-bottom plate with immobilized anti-CD3 (0.05 μg ml^{-1}) plus anti-CD28 (10 μg ml^{-1}) or anti-CD26 (10 μg ml^{-1}) mAbs. After 7 d of stimulation, cell were harvested, mRNA was prepared, and transcript levels of human *IL2*, *IFNG*, *IL17A*, *IL26*, and *DPP4* were quantified by real-time RT-PCR. For IL-26 production analysis via costimulation, 1×10^5 HuCB CD4 T cells were stimulated with plate-bound anti-CD3, anti-CD28, anti-CD26 mAbs, or Cav-Ig immobilized at the indicated concentration. The supernatants were harvested 7 or 14 d after stimulation. For inhibition assay, 1×10^5 cells/well HuCB CD4 T cells were treated with blocking Cav-Ig or control Ig at the various concentrations (0, 1, 5, 10, 20, or 50 μg ml^{-1}) prior to stimulation. After 1-h blocking period, cells were stimulated with immobilized anti-CD3 (0.05 μg ml^{-1}) plus Cav-Ig (20 μg ml^{-1}), anti-CD28 (20 μg ml^{-1}), or anti-CD26 (20 μg ml^{-1}) mAbs. After 7 d of stimulation, the supernatants were harvested. HuCB CD4 T cells were cultured in AIM V serum-free medium (Invitrogen).

Graft-versus-leukemia and bioluminescence imaging

Firefly luciferase-transfected A20 murine lymphoma cells (A20-luc) of BALB/c background ($H\text{-}2^d$) were provided by X. Chen (Medical College of Wisconsin, Milwaukee, WI) (35). NOG mice were irradiated at sublethal dose (200 cGy), inoculated the next day with 1×10^4 A20-luc cells via tail vein, and then transplanted the following day with 1×10^7 MNCs isolated from HuCB. Cav-Ig or control Ig (100 μg/dose) was administered i.p. thrice per week, beginning at day +1 after transplantation until day +28 (total 12 doses). For other graft-versus-leukemia (GVL) experiments, NOG mice were irradiated at sublethal dose (200 cGy), and the next day were transplanted with 1×10^7 MNCs isolated from HuCB. Cav-Ig or control Ig (100 μg/dose) was administered i.p. thrice per week, beginning at day +1 after transplantation until day +28 (total 12 doses). A total of 1×10^5 A20-luc cells was inoculated via tail vein on day +28 posttransplantation. Tumor dissemination was monitored every week using in vivo bioluminescence imaging, as previously described in the literature (36).

Statistics

Data were analyzed by two-tailed Student *t* test for two-group comparison or by ANOVA test for multiple comparison testing, followed by the Tukey-Kramer posthoc test. The *p* values ≤0.05 were considered statistically significant. Survival rates were analyzed by log-rank test using Kaplan–Meier method. Calculations were performed and graphed using GraphPad Prism 6 (GraphPad Software, La Jolla, CA).

Author Manuscript Author Manuscript Author Manuscript Author Manuscript

Study approval

Human study protocols were approved by the Ethics Committees at Juntendo University (authorization number 2012077), and at Keio University (authorization number 20120206). Informed consent was obtained from a patient. Animal experiments were conducted following protocols approved by the Animal Care and Use Committees at Juntendo University (authorization number 1082).

Results

Establishment of obliterative bronchiolitis in mice transplanted with HuCB

As described above, the establishment of a humanized murine model of pulmonary cGVHD is needed to better understand and treat this serious and often fatal complication of alloHSCT. To determine whether pulmonary cGVHD is induced by human immune cells in a murine model, we first attempted to establish a humanized murine model utilizing NOG mice as recipients and HuCB as donor cells. To establish a control that did not develop GVHD following hematopoietic reconstitution, we used T cell–depleted $CD34^+$ cells isolated from HuCB (37–39). As shown in Fig. 1A and Supplemental Fig. 1A, $CD34^+$ transplant mice survived for 5 mo without any sign or symptom of GVHD. Meanwhile, whole CB transplant mice exhibited clinical signs/symptoms of GVHD as early as 4 wk posttransplant (Fig. 1A), and demonstrated significantly decreased survival rate (Supplemental Fig. 1A). Human cells were engrafted similarly in both groups, as shown in Supplemental Fig. 1B. Previous work with other humanized murine models showed that reconstituted human $CD45^+$ cells were overcome by $CD3^+$ T cells posttransplantation due to reduced B cell development (23), which may impair the integrity of host immunity. In contrast, we confirmed that NOG mice transplanted with HuCB maintained a stable number of T and B cells (Supplemental Fig. 1C), consistent with previously reported results (24, 38–40). Therefore, the human immune system appeared to be effectively reconstituted in the present murine model involving whole CB as well as $CD34^+$ transplant. We next conducted histological studies of GVHD target organs. The lung of whole CB transplant mice showed perivascular and subepithelial inflammation and fibrotic narrowing of the bronchiole (Fig. 1B), whereas $CD34^+$ transplant control group displayed normal appearance of GVHD target organs such as the lung (Fig. 1C, *left panel*). For the diagnosis of pulmonary cGVHD, it is necessary to show concomitant active GVHD findings in other organs, including skin and liver (4). Skin of whole CB transplant mice manifested fat loss, follicular dropout, and sclerosis of the reticular dermis in the presence of apoptosis of the basilar keratinocytes, whereas the liver exhibited portal fibrosis and cholestasis (Supplemental Fig. 2). These findings indicate that whole CB transplant mice develop pulmonary cGVHD as well as concomitant active GVHD in skin and liver. Because obliterative bronchiolitis can be characterized as a fibroproliferative disease (7), we also performed Mallory staining and lung collagen assays to quantify collagen contents as a measurement of extent of disease. The lung of whole CB transplant mice displayed a significant increase in peribronchiolar and perivascular collagen deposition and in total lung collagen content, compared with $CD34^+$ transplant mice (Fig. 1C, 1D). Taken together, our data demonstrate that the lung of whole CB transplant mice exhibits obliterative bronchiolitis as manifestation of pulmonary GVHD.

Author Manuscript Author Manuscript Author Manuscript Author Manuscript

To determine the potential cellular mechanisms involved in the pathogenesis of pulmonary GVHD, we next analyzed the composition of human lymphocytes in the GVHD lung. In contrast to data demonstrating that PBL contained human $CD19^+$, $CD33^+$, or $CD56^+$ as well as $CD3^+$ cells (Supplemental Fig. 1C), human $CD3^+$ cells were the predominant cell type observed in the lung of whole CB transplant mice, comprising >99% of the lymphocyte population (Fig. 1E). Moreover, human CD4 T cell subset was predominantly observed compared with CD8 T cells (Fig. 1F). These findings were also confirmed by immunohistochemistry studies of the lung specimens (Fig. 1G). These data suggest that the development of obliterative bronchiolitis found in whole CB transplant mice involves donor-derived human CD3 lymphocytes, particularly CD4 T cells.

IL-26–producing CD4 T cell infiltration in the lung of mice with obliterative bronchiolitis

We next analyzed the expression profile of mRNAs of various inflammatory cytokines in human CD4 T cells isolated from the lung of whole CB transplant mice. As shown in Fig. 2A, *IFNG*, *IL17A*, *IL21*, and *IL26* were significantly increased over the course of GVHD development following whole CB transplantation, whereas *IL2*, *TNF* (TNF-α), *IL4*, *IL6*, and *IL10* were decreased. In addition, substantial increases were seen in levels of *IFNG* and *IL26*, with *IL17A* and *IL21* remaining at a low level. It has been reported that IFN-γ and IL-26 are produced by Th1 cells (41), whereas IFN-γ, IL-17A, and IL-26 are produced by Th17 cells (42). Because both Th1 and Th17 cells strongly express CD26 (15, 43), we next analyzed the expression level of CD26/DPP4. *DPP4* mRNA expression in human CD4 T cells infiltrating in the lung of mice with obliterative bronchiolitis was significantly increased (Fig. 2A).

To determine whether these cytokines were produced by the infiltrating human $CD26^+$CD4 T cells, we next conducted flow cytometric analysis of lymphocytes isolated from the lung of whole CB or $CD34^+$ transplant control mice. As shown in Fig. 2B, levels of human IFN-γ^+ or IL-26^+CD26^+CD4 T cells were significantly increased in whole CB transplant mice as compared with $CD34^+$ transplant control mice, whereas levels of IL-$17A^+CD26^+$CD4 T cells were similarly very low in both groups. These findings were also confirmed by immunohistochemistry studies of the lung specimens (Fig. 2C). To determine whether $CD26^+$CD4 T cells produced IL-26, IFN-γ, and/or IL-17A, multicolor-staining flow cytometric study was conducted. As shown in Fig. 2Di, $CD26^+$CD4 T cells in the lung of whole CB transplant mice predominantly produced IL-26 rather than IFN-γ. In addition, whereas $CD26^+$IFN-γ^+CD4 cells exclusively expressed IL-26, $CD26^+$IL-26^+CD4 cells were predominantly IFN-γ–negative cells, and IL-$17A^+$ cells were exclusively IL-26 negative (Fig. 2Dii). These data suggest that $CD26^+$CD4 T cells in the lung of mice with obliterative bronchiolitis express IL-26 as well as IFN-γ, but do not belong to the Th17 cell population.

To further confirm the above findings, we examined protein levels of the relevant cytokines. In addition, because soluble CD26/DPP4 level is correlated with T cell CD26 protein level and hematopoiesis (44, 45), we examined protein levels of human soluble CD26/DPP4 in murine sera. As shown in Fig. 2E, serum levels of human IFN-γ, IL-26, and human soluble CD26/DPP4 were significantly increased in whole CB transplant mice as compared with $CD34^+$ transplant control mice. Meanwhile, serum levels of human IL-2, IL-4, IL-6, IL-10,

Author Manuscript Author Manuscript Author Manuscript Author Manuscript

IL-17A, and TNF-α were undetectable in both groups (data not shown). Taken together, these findings strongly suggest that IFN-γ^+ and/or IL-26^+CD26^+CD4 T cells play an important role in the pathophysiology of obliterative bronchiolitis after HSCT.

To investigate the role of IL-26^+CD26^+CD4 T cells in humans, we conducted immunohistochemistry studies of a human lung specimen obtained from a patient with cGVHD. A 64-y-old woman underwent an alloPBSCT for ALL after being treated with busulfan, fludarabine, and melphalan as conditioning regimen. Tacrolimus was administered for the prevention of GVHD. The patient developed acute skin GVHD (stage 2 and grade I) on day +33 posttransplant. On day +95, the patient had dyspnea and the chest X-ray revealed ground glass opacity bilaterally. Transbronchial lung biopsy was performed on day +101. Histologic findings of the lung specimen revealed perivascular and subepithelial inflammation and narrowing of the bronchiole with manifestation of peribronchiolar and perivascular collagen deposition (Fig. 2F). The patient was diagnosed as having pulmonary cGVHD with obliterative bronchiolitis. Immunohistochemistry studies showed predominant infiltration of IL-26^+CD26^+CD4 T cells. These findings suggest that IL-26^+CD26^+CD4 T cells play an important role in the pathophysiology of obliterative bronchiolitis after HSCT in human as well as humanized murine model.

Contribution of IL-26 to collagen production in pulmonary GVHD

Because it has been reported that pulmonary GVHD development is independent of IFN-γ (46), we therefore focused on IL-26 as a potential effector cytokine for pulmonary GVHD. As the IL-26 gene is absent in rodents (41, 47), we cannot formally exclude the possibility that human IL-26 activates murine cells. We therefore conducted in vitro assays to determine the effect of human IL-26 on murine cells. In human cells, IL-26 binds initially to IL-20RA to form the binary complex IL-26 plus IL-20RA, followed by recruitment of the IL-10RB chain, leading to STAT3 phosphorylation (26). We thus confirmed that both IL-20RA and IL-10RB were expressed in murine fibroblast cell line NIH3T3 as well as NHLF (Fig. 3A, 3B). In both NHLF and NIH3T3, exogenous human rIL-26 induced phosphorylation of STAT3 (Fig. 3C), indicating that human IL-26 was active not only in NHLF, but also in murine fibroblast. To examine a functional effect of IL-26 on murine fibroblasts, we next conducted an in vitro assay for collagen production. As shown in Fig. 3D, increased levels of collagen production in NIH3T3 as well as in NHLF were observed in a dose-dependent manner following the addition of exogenous IL-26, and collagen production was inhibited by neutralizing anti–IL-20RA pAb. These results strongly suggest that human IL-26 activates both human and murine fibroblasts via IL-20RA, leading to increased collagen production.

To further extend the above in vitro results to an in vivo system, we analyzed the lung of murine alloreactive GVHD using human *IL26* Tg mice. For this purpose, we used mice carrying human *IFNG* and *IL26* transgene (190-*IFNG* Tg mice) or mice carrying human IFNG transgene with deleting *IL26* transcription (ΔCNS-77 Tg mice). The 190-*IFNG* Tg mice exhibited production of IL-26 by CD4 T cells under Th1- or Th17-polarizing conditions, whereas expression of IL-26 was completely abrogated in ΔCNS-77 Tg mice (41). In addition, production of IFN-γ by T or NK cells was equivalent in both 190-*IFNG* Tg

Author Manuscript Author Manuscript Author Manuscript Author Manuscript

and ΔCNS-77 Tg mice (28). As shown in Fig. 3E, lung histology of recipient NOG mice deriving from B6 wild-type or ΔCNS-77 Tg mice showed peribronchial infiltration and cuffing denoting GVHD, whereas collagen deposit was not detected by Mallory staining, and IL-26$^+$ cells were not detected. In contrast, histology of recipient NOG mice deriving from 190-*IFNG* Tg mice showed peribronchial infiltration and cuffing denoting GVHD with collagen deposition and IL-26$^+$ cell infiltration. Significant increase in collagen contents of the lung of recipient NOG mice deriving from 190-IFNG Tg mice was noted (Fig. 3F). These results suggest that human IL-26, but not human IFN-γ, plays a critical role in the pulmonary fibrosis associated with obliterative bronchiolitis after HSCT.

To further define the role of IL-26 in the pulmonary fibrosis associated with HSCT, we conducted studies to evaluate whether lung collagen contents were reduced by neutralizing IL-26 in whole CB transplant mice. For this purpose, anti–IL-26 pAb or control pAb was administered in sublethally irradiated NOG mice transplanted with whole CB on day +21 until day +32 thrice per week, followed by resection of the lung to measure total collagen content. As shown in Fig. 3G, a significant decrease in collagen contents of the lung of recipient NOG mice treated with anti–IL-26 pAb was noted. Taken together, our data strongly suggest that IL-26 plays a critical role in the pulmonary fibrosis observed following HSCT.

IL-26 production via CD26-mediated T cell costimulation

IL-26 was preferentially expressed in CD26$^+$CD4 T cells in the lung of whole CB transplant mice experiencing obliterative bronchiolitis (Fig. 2D), with increased expression of *DPP4* (Fig. 2A). Although upstream stimulation of IL-26 synthesis has not yet been determined, CD26/DPP4 as well as IFN-γ is preferentially expressed on Th1 cells activated via CD26-mediated costimulation (15). We thus hypothesized that human CD4 T cells produce IL-26 following CD26 costimulation. To test this hypothesis, we conducted in vitro costimulatory experiments using HuCB CD4 T cells and analyzed expression of various inflammatory cytokines. As shown in Fig. 4A, although expression levels of *IL26* and *DPP4* were enhanced by CD28 (*) or CD26 (**) costimulation, significantly greater increase in levels of *IL26* and *DPP4* was observed following CD26 costimulation than CD28 costimulation (***). In contrast, expression levels of *IL2*, *IFNG*, and *IL17A* were not increased following either CD26 costimulation or CD28 costimulation (Fig. 4A), due to the immaturity of HuCB T cells, as was previously reported (21, 48). We next conducted costimulatory experiments evaluating dose effect and time kinetics using the CD26 costimulatory ligand Cav-Ig as well as anti-CD26 or anti-CD28 mAbs, and assayed for secreted IL-26. As shown in Fig. 4B, production of IL-26 was increased following CD26 costimulation with Cav-Ig (*) or anti-CD26 (**) mAb in dose- and time-dependent manners, whereas a slight increase in IL-26 level was observed following CD28 costimulation only at higher doses of mAb and longer stimulation periods (***). Blocking experiments were then performed for further confirmation, showing that IL-26 production induced by Cav-Ig or anti-CD26 mAb was clearly inhibited by treatment with soluble Cav-Ig in a dose-dependent manner (Fig. 4C), whereas no change was observed with CD28 costimulation (Fig. 4C). These findings strongly suggest that production of IL-26 by HuCB CD4 T cells is regulated via CD26-mediated co-stimulation. Moreover, because the functional sequences of the N-terminal of

Author Manuscript Author Manuscript Author Manuscript Author Manuscript

caveolin-1 are highly conserved between human and mouse (49), allowing for the capability to bind human CD26 as a costimulatory ligand, it is conceivable that donor HuCB T cells transferred into mice were activated via CD26 costimulation triggered by murine caveolin-1. Taken together, CD26-mediated IL-26 production triggered by caveolin-1 is identified as a possible therapeutic target in pulmonary cGVHD through the use of whole CB transplant mice.

Prevention of obliterative bronchiolitis in whole CB transplant mice by Cav-Ig administration

Given the role of CD26 costimulation in IL-26 production and IL-26 regulation of collagen production, we therefore sought to determine whether disruption of CD26 costimulation by a blocking reagent, Cav-Ig, prolonged survival of the recipient mice associated with a reduction in the incidence of obliterative bronchiolitis. Recipients treated with Cav-Ig survived for 7 mo without any clinical findings of GVHD (Fig. 5A, 5B). Meanwhile, the survival rate of recipient mice treated with control Ig was significantly reduced (Fig. 5A), with clinical signs/symptoms of GVHD (Fig. 5B). Human cells were engrafted similarly in both groups, as shown in Supplemental Fig. 3A, 3B. Histologic findings of the lung showed the development of obliterative bronchiolitis in control Ig, while having normal appearances in Cav-Ig recipient mice, with none having positive pathology scores (Fig. 5C, 5D). These effects of Cav-Ig were also observed in other GVHD-target organs such as the skin and liver (Supplemental Fig. 3C). Moreover, IL-26^{+}CD26^{+}CD4 T cells in the lung and serum levels of human IL-26 and soluble CD26/DPP4 were significantly decreased in Cav-Ig–administered recipients than in control Ig (Fig. 5E, 5F). Furthermore, collagen contents in the lung were reduced in Cav-Ig–administered recipients (Fig. 5G, 5H). Taken together, the above results support the notion that Cav-Ig administration prevents the development of pulmonary GVHD in whole CB transplant mice by decreasing the number of IL-26^{+}CD26^{+}CD4 T cells.

Effect of Cav-Ig administration after onset of GVHD

Because pulmonary GVHD progresses in an indolent manner over weeks and months, patients often are affected by the clinical findings prior to being diagnosed with cGVHD (50). We therefore sought to determine whether blockade of caveolin-1/CD26 interaction effectively suppresses obliterative bronchiolitis development following the appearance of clinical signs/symptoms. For this purpose, treatment began on day +29 following the appearance of an increase in GVHD scores, indicating the early stages of cGVHD development. Recipients treated with Cav-Ig survived for 7 mo with remission of GVHD symptoms (Fig. 6A, 6B). Meanwhile, the survival rate of recipients treated with control Ig was significantly decreased (Fig. 6A), with progression of clinical signs/symptoms of GVHD (Fig. 6B). Human cells were engrafted similarly in both groups (Supplemental Fig. 4A, 4B). In contrast to progressive obliterative bronchiolitis of control Ig-treated recipients, peribronchial inflammation shown at 5 wk posttransplantation was attenuated at 10 wk posttransplantation in Cav-Ig–treated recipients (Fig. 6C). Correspondingly, the pathologic scores of control Ig-treated recipients were significantly increased at 10 wk, as compared with those at 5 wk (Fig. 6D). Meanwhile, the pathologic scores of Cav-Ig–treated recipients were significantly reduced at 10 wk, as compared with those at 5 wk (Fig. 6D), and were

Author Manuscript Author Manuscript Author Manuscript Author Manuscript

clearly decreased as compared with those of control Ig-treated recipients (Fig. 6D). These effects of Cav-Ig administration were observed in the skin and liver (Supplemental Fig. 4C–F). Moreover, levels of human IFN-γ^+ and IL-26^+CD26^+CD4 T cells in the lung of control Ig-treated recipients were significantly increased at 10 wk, as compared with those at 5 wk (* of Fig. 6E). In contrast, levels of human IFN-γ^+ and IL-26^+CD26^+CD4 T cells in the lung of Cav-Ig–treated recipients were significantly reduced at 10 wk, as compared with those at 5 wk (** of Fig. 6E), and were clearly decreased as compared with those of control Ig-treated recipients (*** of Fig. 6E). Furthermore, total collagen contents in the lung were significantly lower in Cav-Ig–treated recipients than control Ig-treated recipients (Fig. 6F). Taken together, these data suggest that Cav-Ig administration not only prevents the development of cGVHD, but also provides a novel therapeutic approach for the early stages of cGVHD by regulating levels of IL-26^+CD26^+CD4 T cells.

Treatment with Cav-Ig preserves GVL capability in recipient mice

Because GVHD and GVL effects are highly linked immune reactions (51), we evaluated the potential influence of Cav-Ig treatment on GVL effect. For this purpose, cohorts of Cav-Ig—or control Ig-treated recipient mice of whole CB transplant were irradiated at sublethal doses and then injected i.v. with luciferase-transfected A20 (A20-luc) cells 1 d prior to whole CB transplantation to allow for dissemination of tumor cells. The next day following transplantation, treatment with Cav-Ig or control Ig thrice per week began on day +1 until day +28. Mice inoculated with A20 cells alone all died of tumor progression within 6 wk (Fig. 7A, 7B). Recipients treated with control Ig exhibited clinical evidence of GVHD such as weight loss and ruffled fur and died of GVHD without tumor progression in 13 wk (Fig. 7A, 7B). In contrast, recipient mice treated with Cav-Ig displayed significantly prolonged survival (Fig. 7A) without involvement of A20-luc cells (Fig. 7B). To better characterize the potency of the GVL effect, we repeated these studies with injection of A20-luc cells on day +28 after whole CB transplantation to allow for acquisition of immunosuppression by Cav-Ig treatment. Mice inoculated with A20 cells alone all died of tumor progression within 2 wk after tumor inoculation (Fig. 7C, 7D). Recipient mice treated with control Ig demonstrated clinical evidence of GVHD such as weight loss and ruffled fur and died of GVHD without tumor progression within 13 wk after transplantation (Fig. 7C, 7D). In contrast, recipients treated with Cav-Ig exhibited significantly prolonged survival (Fig. 7C) without involvement of A20-luc cells (Fig. 7D). Collectively, these results demonstrate that Cav-Ig treatment of recipient mice of whole CB transplant was effective in reducing the symptoms of cGVHD without a concomitant loss of the GVL effect.

Discussion

In the current study, we demonstrated that obliterative bronchiolitis developed in NOG mice transplanted with HuCB (whole CB transplant). Utilizing this humanized mouse model, we found that donor-derived CD4 T cells predominantly infiltrated in the lung of obliterative bronchiolitis, and that IL-26 as well as IFN-γ levels were enhanced significantly in the infiltrating human $CD26^+$CD4 T cells.

Author Manuscript Author Manuscript Author Manuscript Author Manuscript

Originally discovered in *Herpesvirus saimiri*–transformed T cells (52), IL-26 is now classified as belonging to the IL-10 family of cytokines (42). IL-26 is a secreted protein produced by T, NK cells, or synoviocytes (53, 54), and binding of IL-26 to a distinct cell surface receptor consisting of IL-20RA and IL-10RB results in functional activation via STAT3 phosphorylation (26). IL-26 gene expression or protein production has been analyzed in patients with RA, inflammatory bowel diseases, and hepatitis C virus infection (54–58). However, the effect of IL-26 on the pathophysiology of cGVHD has not yet been determined. Moreover, there has been little information available regarding the biological functions of IL-26 using animal models due to the absence of the IL-26 gene in mouse (41, 47). In this study, we described a novel effect of IL-26 on fibroproliferation in transplant-related obliterative bronchiolitis, using a humanized pulmonary cGVHD murine model. Moreover, we demonstrated that human IL-26, not IFN-γ, induced collagen deposition in obliterative bronchiolitis of murine allogeneic transplantation model utilizing 190-*IFNG* Tg and ΔCNS-77 Tg mice. In both 190-*IFNG* Tg and ΔCNS-77 Tg mice, production of IFN-γ by T or NK cells is equivalent in both tissue culture studies and analysis of basal levels in various tissues, including spleen, lymph node, and colon (28). In contrast, expression of IL-26 is observed in Th1- or Th17-polarizing CD4 cells of 190-*IFNG* Tg mice, whereas it is completely abrogated in ΔCNS-77 Tg mice (41). Moreover, IFN-γ^+CD4 T cells infiltrating in the lung of obliterative bronchiolitis exclusively expressed IL-26, whereas IL-17A$^+$CD4 T cells were negative for IL-26. To characterize the role of IL-26$^+$CD26$^+$CD4 T cells in patients with obliterative bronchiolitis, we analyzed the lung specimen of a patient with dyspnea and ground glass opacity detected on the chest X-ray examination on day +95 of alloPBSCT for ALL. Although a limited number of samples was obtained because invasive examinations including lung biopsy are not necessary to diagnose lung cGVHD (4), our data obtained from a human lung sample confirm the findings shown in the above murine model. Collectively, our data imply that IL-26$^+$CD26$^+$ Th1 cells play an important role in the pathogenesis of obliterative bronchiolitis observed in a cGVHD patient as well as in whole CB transplant mice. Regarding its specific receptor, IL-26 primarily binds to IL-20RA, followed by recruitment of IL-10RB (26). Although IL-10RB is broadly expressed on most cell types and tissues, IL-20RA is not expressed in lymphoid organs, but is expressed in the lung as well as skin (59). It is thus conceivable that IL-26–related fibroproliferation occurs in the lung and skin.

It has been reported that allogeneic Th17 cells could induce severe forms of acute GVHD associated with cutaneous and pulmonary pathologic manifestations (60). Moreover, in studies of lung transplant recipients using murine model and human samples, IL-17 was shown to be involved in the pathogenesis of obliterative bronchiolitis associated with chronic rejection (61, 62). In the current study, we demonstrated that levels of *IL17A* and IL-17–producing cells were slightly increased in CD4 T cells infiltrating the obliterative bronchiolitis lung. Although the role of IL-17 in cGVHD is still unclear (63), we could not exclude the possibility that small populations of IL-17$^+$CD4 T cells are involved in the pathogenesis of obliterative bronchiolitis in cGVHD. In addition, Th17 cells display a great degree of context-dependent plasticity, as they are capable of acquiring functional characteristics of Th1 cells (64). This late plasticity may play a role in the development of

Author Manuscript Author Manuscript Author Manuscript Author Manuscript

obliterative bronchiolitis regulated by $CD26^+$CD4 Th1 cells, and may be associated with the emergence of IL-26^+CD26^+ Th1 cells.

Several causes of obliterative bronchiolitis after alloHSCT have been proposed, including donor-derived T cell–mediated injury, several profibrotic factors, and autoantibody deposition (7). Recent report using a murine model showed that donor-derived B cell activation and maturation with the aid of T follicular helper cells were necessary for cGVHD, and bronchiolitis obliterans syndrome was reversed by the abrogation of IL-21 signaling (65). However, our present model using human donor cells did not demonstrate the presence of B cells in the lung of obliterative bronchiolitis, whereas a substantial B cell population was detected in the recipient PBL. In fact, no direct evidence for a causal relationship for autoantibodies or alloantibodies in the pathogenesis of organ manifestation of cGVHD has been observed in humans (9). Furthermore, cGVHD of the visceral organs seemed to respond poorly to B cell depletion therapy such as rituximab (7, 9). It is speculated that this observed discrepancy is due to differences in the B cell maturation process between mice and humans (11). Despite these limitations of murine or humanized murine models, targeting CD4 T cells to control cGVHD is a reasonable therapeutic approach because T cell help plays a pivotal role in B cell maturation and activation in cGVHD (66).

A related issue concerns the process of B cell development in humanized mice. Previous work has shown that reconstituted human $CD45^+$ cells in other models of humanized mice were overcome by $CD3^+$ T cells within several months of transplantation due to reduced B cell development (40). However, given the fact that HuCB contains ample HSC as well as naive lymphocytes, the use of HuCB as donor cells led to sustained recovery of lymphocytes in the recipient PBL, as had also been reported by other investigators (24, 38, 39, 67). In addition, it has been demonstrated that specific Abs in human B cells generated in the humanized mice transplanted with HSC isolated from HuCB are effectively synthesized (23, 24, 38, 40). A potential concern regarding the applicability of results obtained from our model is the lack of intestinal GVHD. Because recent work demonstrated that neutrophils play an important role in intestinal GVHD (68), one possible explanation for the lack of intestinal GVHD in our model is that achieving effective engraftment of neutrophils in our model is particularly difficult (40). Despite the limitations of cross-species comparisons, our study provides insights into the pathogenesis of clinical pulmonary cGVHD induced by human lymphocytes. Furthermore, data obtained from our study have identified potential novel therapeutic targets in the management of clinical cGVHD.

Because we previously showed an effectiveness of anti-CD26 mAb on an aGVHD model using adult PBL (13), we performed preliminary testing of anti-CD26 mAb effect on recipient mice of whole CB transplant, and found a high incidence of graft failure (data not shown). Our speculation of the reason for this failure is as follows: we previously reported that HuCB CD4 T cells broadly express CD26 (21), and other investigators observed that $CD34^+CD38^{low/-}$ or $CD34^+CD38^+$ hematopoietic stem/progenitor cells in HuCB preferentially express CD26 (69). These findings suggest that treatment with anti-CD26 mAb in a HuCB transplant model may reduce the levels of hematopoietic stem/progenitor and/or CD4 T cells in the graft of HuCB, resulting in increased graft failure. Meanwhile, it

Author Manuscript Author Manuscript Author Manuscript Author Manuscript

has been reported that endogenous CD26 expression on donor cells negatively regulates homing and engraftment (70), and that inhibition of DPP4 enzyme activity enhances engraftment of hematopoietic cells in mice and humans (71, 72). In the current study, we observed no difference of engraftment between Cav-Ig– and control Ig-treated mice. It is conceivable that continuous inhibition of DPP4 enzyme activity was not achieved by the alternate-day schedule of administration of Cav-Ig used in the current study, with the resultant lack of continuous inhibition of related chemokines, cytokines, and CSFs (71).

In addition to issues involving the use of anti-CD26 mAb, it is important to point out that there may be potential adverse events such as off-target effects associated with the proposed use of Cav-Ig therapy. Although caveolin-1 exists in the inner surface of most cell types (49), its N terminus is detected on endothelial cells as well as APCs after activation (73). Therefore, it is possible that Cav-Ig binds to cell surface caveolin-1 and is consumed in such endothelial cells. Other issues relate to the GVL effects. Our data demonstrated that Cav-Ig clearly impeded GVHD in our model with preservation of GVL effects. We speculate that CD26-dependent xenogeneic priming of CD4 T cells is inhibited by Cav-Ig (13, 20), whereas CD28-dependent GVL effects are exerted after engraftment (74). However, studying GVHD and GVL effects that require similar CD4- or CD8-dependent pathways with the use of primary leukemic cells rather than cell lines should help to generate reliable models of GVL. Despite these concerns, our work revealed no abnormal findings in the vessels and organs of Cav-Ig–treated recipient mice with preservation of the GVL effect, hence suggesting a potentially promising novel therapeutic approach for controlling cGVHD.

The administration of Cav-Ig may potentially result in renal damage because CD26 is also expressed in the kidney (44, 45). However, we observed no pathological changes in the kidney in mice treated with Cav-Ig (data not shown). These findings may be partially due to the fact that CD26 in the kidney is mainly expressed in the proximal tubules (75), and that immune complex deposition of complexes consisting of Cav-Ig and membrane-bound CD26 did not occur in the glomeruli to cause renal injury.

In conclusion, our present work demonstrates that caveolin-1 blockade can control pulmonary GVHD by suppressing the immune functions of donor-derived T cells and decreasing IL-26 production. Moreover, IL-26^{+}CD26^{+}CD4 T cell infiltration appears to play a significant role in the lung of obliterative bronchiolitis. Although complete suppression of cGVHD with current interventional strategies represents a difficult challenge at the present time, our data demonstrate that control of cGVHD clinical findings can be achieved in a murine experimental system by regulating IL-26^{+}CD26^{+}CD4 T cells with Cav-Ig. Our work also suggests that Cav-Ig treatment may be a novel therapeutic approach for chronic inflammatory diseases, including RA and inflammatory bowel diseases, in which IL-26 plays an important role.

Supplementary Material

Refer to Web version on PubMed Central for supplementary material.

Author Manuscript Author Manuscript Author Manuscript Author Manuscript

Acknowledgments

This work was supported in part by a grant from the Ministry of Education, Science, Sports, and Culture, Japan (to K.O. and CM.); a grant from the Ministry of Health, Labour, and Welfare, Japan (to CM.); a grant-in-aid (S1311011) from the Foundation of Strategic Research Projects in Private Universities from the Ministry of Education, Culture, Sports, Science, and Technology, Japan (to K.O. and CM.); and National Institutes of Health Grant RO1 AI044924 (to T.M.A.).

Abbreviations in this article

aGVHD	acute GVHD
ALL	acute lymphoblastic leukemia
alloHSCT	allogeneic hematopoietic stem cell transplantation
alloPBSCT	allogeneic peripheral blood-stem cell transplant
B6	C57BL/6
BAC	bacterial artificial chromosome
Cav-Ig	Ig Fc domain fused with the N-terminal of caveolin-1
cGVHD	chronic GVHD
CNS	conserved noncoding sequence
DPP4	dipeptidyl peptidase IV
GVHD	graft-versus-host disease
GVL	graft-versus-leukemia
HPRT1	hypoxanthine phosphoribosyltransferase 1
HSC	hematopoietic stem cell
HuCB	human umbilical cord blood
MNC	mononuclear cell
NHLF	normal human lung fibroblast
pAb	polyclonal Ab
RA	rheumatoid arthritis
RIPA	radioimmunoprecipitation assay
Tg	transgenic

References

1. Champlin RE, Schmitz N, Horowitz MM, Chapuis B, Chopra R, Cornelissen JJ, Gale RP, Goldman JM, Loberiza FR Jr, Hertenstein B, et al. Blood stem cells compared with bone marrow as a source of hematopoietic cells for allogeneic transplantation. Blood. 2000; 95:3702–3709. [PubMed: 10845900]
2. Socié G, Ritz J. Current issues in chronic graft-versus-host disease. Blood. 2014; 124:374–384. [PubMed: 24914139]

Author Manuscript Author Manuscript Author Manuscript Author Manuscript

3. Baird K, Pavletic SZ. Chronic graft versus host disease. Curr Opin Hematol. 2006; 13:426–435. [PubMed: 17053454]
4. Filipovich AH, Weisdorf D, Pavletic S, Socie G, Wingard JR, Lee SJ, Martin P, Chien J, Przepiorka D, Couriel D, et al. National Institutes of Health consensus development project on criteria for clinical trials in chronic graft-versus-host disease: I. Diagnosis and staging working group report. Biol Blood Marrow Transplant. 2005; 11:945–956. [PubMed: 16338616]
5. Bergeron A, Godet C, Chevret S, Lorillon G, Peffault de Latour R, de Revel T, Robin M, Ribaud P, Socié G, Tazi A. Bronchiolitis obliterans syndrome after allogeneic hematopoietic SCT: phenotypes and prognosis. Bone Marrow Transplant. 2013; 48:819–824. [PubMed: 23208317]
6. Chu YW, Gress RE. Murine models of chronic graft-versus-host disease: insights and unresolved issues. Biol Blood Marrow Transplant. 2008; 14:365–378. [PubMed: 18342778]
7. Barker AF, Bergeron A, Rom WN, Hertz MI. Obliterative bronchiolitis. N Engl J Med. 2014; 370:1820–1828. [PubMed: 24806161]
8. Reddy P, Johnson K, Uberti JP, Reynolds C, Silver S, Ayash L, Braun TM, Ratanatharathorn V. Nephrotic syndrome associated with chronic graft-versus-host disease after allogeneic hematopoietic stem cell transplantation. Bone Marrow Transplant. 2006; 38:351–357. [PubMed: 16862167]
9. Shimabukuro-Vornhagen A, Hallek MJ, Storb RF, von Bergwelt-Baildon MS. The role of B cells in the pathogenesis of graft-versus-host disease. Blood. 2009; 114:4919–4927. [PubMed: 19749094]
10. Seok J, Warren HS, Cuenca AG, Mindrinos MN, Baker HV, Xu W, Richards DR, McDonald-Smith GP, Gao H, Hennessy L, et al. Genomic responses in mouse models poorly mimic human inflammatory diseases. Proc Natl Acad Sci USA. 2013; 110:3507–3512. [PubMed: 23401516]
11. Benitez A, Weldon AJ, Tatosyan L, Velkuru V, Lee S, Milford TA, Francis OL, Hsu S, Nazeri K, Casiano CM, et al. Differences in mouse and human nonmemory B cell pools. J Immunol. 2014; 192:4610–4619. [PubMed: 24719464]
12. Antin JH, Bierer BE, Smith BR, Ferrara J, Guinan EC, Sieff C, Golan DE, Macklis RM, Tarbell NJ, Lynch E, et al. Selective depletion of bone marrow T lymphocytes with anti-CD5 monoclonal antibodies: effective prophylaxis for graft-versus-host disease in patients with hematologic malignancies. Blood. 1991; 78:2139–2149. [PubMed: 1717080]
13. Hatano R, Ohnuma K, Yamamoto J, Dang NH, Yamada T, Morimoto C. Prevention of acute graft-versus-host disease by humanized anti-CD26 monoclonal antibody. Br J Haematol. 2013; 162:263–277. [PubMed: 23692598]
14. Fox DA, Hussey RE, Fitzgerald KA, Acuto O, Poole C, Palley L, Daley JF, Schlossmanand SF, Reinherz EL. Ta1, a novel 105 KD human T cell activation antigen defined by a monoclonal antibody. J Immunol. 1984; 133:1250–1256. [PubMed: 6205075]
15. Morimoto C, Schlossman SF. The structure and function of CD26 in the T-cell immune response. Immunol Rev. 1998; 161:55–70. [PubMed: 9553764]
16. Ohnuma K, Dangand NH, Morimoto C. Revisiting an old acquaintance: CD26 and its molecular mechanisms in T cell function. Trends Immunol. 2008; 29:295–301. [PubMed: 18456553]
17. Ohnuma K, Hosono O, Dang NH, Morimoto C. Dipeptidyl peptidase in autoimmune pathophysiology. Adv Clin Chem. 2011; 53:51–84. [PubMed: 21404914]
18. Ohnuma K, Munakata Y, Ishii T, Iwata S, Kobayashi S, Hosono O, Kawasaki H, Dangand NH, Morimoto C. Soluble CD26/dipeptidyl peptidase IV induces T cell proliferation through CD86 up-regulation on APCs. J Immunol. 2001; 167:6745–6755. [PubMed: 11739489]
19. Ohnuma K, Yamochi T, Uchiyama M, Nishibashi K, Yoshikawa N, Shimizu N, Iwata S, Tanaka H, Dang NH, Morimoto C. CD26 up-regulates expression of CD86 on antigen-presenting cells by means of caveolin-1. Proc Natl Acad Sci USA. 2004; 101:14186–14191. [PubMed: 15353589]
20. Ohnuma K, Uchiyama M, Hatano R, Takasawa W, Endo Y, Dangand NH, Morimoto C. Blockade of CD26-mediated T cell costimulation with soluble caveolin-1-Ig fusion protein induces anergy in $CD4^{+}$T cells. Biochem Biophys Res Commun. 2009; 386:327–332. [PubMed: 19523449]
21. Kobayashi S, Ohnuma K, Uchiyama M, Iino K, Iwata S, Dangand NH, Morimoto C. Association of CD26 with CD45RA outside lipid rafts attenuates cord blood T-cell activation. Blood. 2004; 103:1002–1010. [PubMed: 14525771]

Author Manuscript Author Manuscript Author Manuscript Author Manuscript

22. Sato K, Nagayamaand H, Takahashi TA. Aberrant CD3- and CD28-mediated signaling events in cord blood T cells are associated with dysfunctional regulation of Fas ligand-mediated cytotoxicity. J Immunol. 1999; 162:4464–4471. [PubMed: 10201983]
23. Shultz LD, Brehm MA, Garcia-Martinez JV, Greiner DL. Humanized mice for immune system investigation: progress, promise and challenges. Nat Rev Immunol. 2012; 12:786–798. [PubMed: 23059428]
24. Tezuka K, Xun R, Tei M, Ueno T, Tanaka M, Takenouchiand N, Fujisawa J. An animal model of adult T-cell leukemia: humanized mice with HTLV-1-specific immunity. Blood. 2014; 123:346–355. [PubMed: 24196073]
25. Morimoto C, Torimoto Y, Levinson G, Rudd CE, Schrieber M, Dang NH, Letvin NL, Schlossman SF. 1F7, a novel cell surface molecule, involved in helper function of CD4 cells. J Immunol. 1989; 143:3430–3439. [PubMed: 2479677]
26. Ho¨r S, Pirzer H, Dumoutier L, Bauer F, Wittmann S, Sticht H, Renauld JC, de Waal Malefytand R, Fickenscher H. The T-cell lymphokine interleukin-26 targets epithelial cells through the interleukin-20 receptor 1 and interleukin-10 receptor 2 chains. J Biol Chem. 2004; 279:33343–33351. [PubMed: 15178681]
27. Ohnuma K, Uchiyama M, Yamochi T, Nishibashi K, Hosono O, Takahashi N, Kina S, Tanaka H, Lin X, Dangand NH, Morimoto C. Caveolin-1 triggers T-cell activation via CD26 in association with CARMA1. J Biol Chem. 2007; 282:10117–10131. [PubMed: 17287217]
28. Collins PL, Chang S, Henderson M, Soutto M, Davis GM, McLoed AG, Townsend MJ, Glimcher LH, Mortlock DP, Aune TM. Distal regions of the human IFNG locus direct cell type-specific expression. J Immunol. 2010; 185:1492–1501. [PubMed: 20574006]
29. Cooke KR, Kobzik L, Martin TR, Brewer J, Delmonte J Jr, Crawfordand JM, Ferrara JL. An experimental model of idiopathic pneumonia syndrome after bone marrow transplantation: I. The roles of minor H antigens and endotoxin. Blood. 1996; 88:3230–3239. [PubMed: 8963063]
30. Anderson BE, McNiff JM, Matte C, Athanasiadis I, Shlomchik WD, Shlomchik MJ. Recipient $CD4^+$ T cells that survive irradiation regulate chronic graft-versus-host disease. Blood. 2004; 104:1565–1573. [PubMed: 15150080]
31. Kaplan DH, Anderson BE, McNiff JM, Jain D, Shlomchik MJ, Shlomchik WD. Target antigens determine graft-versus-host disease phenotype. J Immunol. 2004; 173:5467–5475. [PubMed: 15494494]
32. Aoe K, Amatya VJ, Fujimoto N, Ohnuma K, Hosono O, Hiraki A, Fujii M, Yamada T, Dang NH, Takeshima Y, et al. CD26 overexpression is associated with prolonged survival and enhanced chemosensitivity in malignant pleural mesothelioma. Clin Cancer Res. 2012; 18:1447–1456. [PubMed: 22261805]
33. Hatano R, Ohnuma K, Yamamoto J, Dangand NH, Morimoto C. CD26-mediated co-stimulation in human $CD8^+$ T cells provokes effector function via pro-inflammatory cytokine production. Immunology. 2013; 138:165–172. [PubMed: 23113658]
34. Ohnuma K, Saito T, Hatano R, Hosono O, Iwata S, Dang NH, Ninomiya H, Morimoto C. Comparison of two commercial ELISAs against an in-house ELISA for measuring soluble CD26 in human serum. J Clin Lab Anal. 201410.1002/jcla.21736
35. Chen X, Dodge J, Komorowski R, Drobyski WR. A critical role for the retinoic acid signaling pathway in the pathophysiology of gastrointestinal graft-versus-host disease. Blood. 2013; 121:3970–3980. [PubMed: 23529927]
36. Yamamoto J, Ohnuma K, Hatano R, Okamoto T, Komiya E, Yamazaki H, Iwata S, Dang NH, Aoe K, Kishimoto T, et al. Regulation of somatostatin receptor 4-mediated cytostatic effects by CD26 in malignant pleural mesothelioma. Br J Cancer. 2014; 110:2232–2245. [PubMed: 24743707]
37. Ito M, Hiramatsu H, Kobayashi K, Suzue K, Kawahata M, Hioki K, Ueyama Y, Koyanagi Y, Sugamura K, Tsuji K, et al. NOD/SCID/γc^{null} mouse: an excellent recipient mouse model for engraftment of human cells. Blood. 2002; 100:3175–3182. [PubMed: 12384415]
38. Matsumura T, Kametani Y, Ando K, Hirano Y, Katano I, Ito R, Shiina M, Tsukamoto H, Saito Y, Tokuda Y, et al. Functional $CD5^+$ B cells develop predominantly in the spleen of NOD/SCID/γc^{null} (NOG) mice transplanted either with human umbilical cord blood, bone marrow, or mobilized peripheral blood CD34+ cells. Exp Hematol. 2003; 31:789–797. [PubMed: 12962725]

Author Manuscript Author Manuscript Author Manuscript Author Manuscript

39. Yahata T, Ando K, Nakamura Y, Ueyama Y, Shimamura K, Tamaoki N, Kato S, Hotta T. Functional human T lymphocyte development from cord blood $CD34^+$ cells in nonobese diabetic/Shi-*scid*, IL-2 receptor γ null mice. J Immunol. 2002; 169:204–209. [PubMed: 12077246]
40. Ito R, Takahashi T, Katano I, Ito M. Current advances in humanized mouse models. Cell Mol Immunol. 2012; 9:208–214. [PubMed: 22327211]
41. Collins PL, Hendersonand MA, Aune TM. Lineage-specific adjacent IFNG and IL26 genes share a common distal enhancer element. Genes Immun. 2012; 13:481–488. [PubMed: 22622197]
42. Donnelly RP, Sheikh F, Dickensheets H, Savan R, Young HA, Walter MR. Interleukin-26: an IL-10-related cytokine produced by Th17 cells. Cytokine Growth Factor Rev. 2010; 21:393–401. [PubMed: 20947410]
43. Bengsch B, Seigel B, Flecken T, Wolanski J, Blum HE, Thimme R. Human Th17 cells express high levels of enzymatically active dipeptidylpeptidase IV (CD26). J Immunol. 2012; 188:5438–5447. [PubMed: 22539793]
44. Gorrell MD, Gysbersand V, McCaughan GW. CD26: a multifunctional integral membrane and secreted protein of activated lymphocytes. Scand J Immunol. 2001; 54:249–264. [PubMed: 11555388]
45. Wang Z, Grigo C, Steinbeck J, von Hörsten S, Amann K, Daniel C. Soluble DPP4 originates in part from bone marrow cells and not from the kidney. Peptides. 2014; 57:109–117. [PubMed: 24874705]
46. Yi T, Chen Y, Wang L, Du G, Huang D, Zhao D, Johnston H, Young J, Todorov I, Umetsu DT, et al. Reciprocal differentiation and tissue-specific pathogenesis of Th1, Th2, and Th17 cells in graft-versus-host disease. Blood. 2009; 114:3101–3112. [PubMed: 19602708]
47. Fickenscher H, Pirzer H. Interleukin-26. Int Immunopharmacol. 2004; 4:609–613. [PubMed: 15120646]
48. Kloosterboer FM, van Luxemburg-Heijs SA, Willemze R, Falkenburg JH. Similar potential to become activated and proliferate but differential kinetics and profiles of cytokine production of umbilical cord blood T cells and adult blood naive and memory T cells. Hum Immunol. 2006; 67:874–883. [PubMed: 17145367]
49. Engelman JA, Zhang X, Galbiati F, Volonte D, Sotgia F, Pestell RG, Minetti C, Scherer PE, Okamoto T, Lisanti MP. Molecular genetics of the caveolin gene family: implications for human cancers, diabetes, Alzheimer disease, and muscular dystrophy. Am J Hum Genet. 1998; 63:1578–1587. [PubMed: 9837809]
50. Soiffer R. Immune modulation and chronic graft-versus-host disease. Bone Marrow Transplant. 2008; 42(Suppl 1):S66–S69. [PubMed: 18724307]
51. Wu CJ, Ritz J. Revealing tumor immunity after hematopoietic stem cell transplantation. Clin Cancer Res. 2009; 15:4515–4517. [PubMed: 19584145]
52. Knappe A, Ho¨r S, Wittmann S, Fickenscher H. Induction of a novel cellular homolog of interleukin-10, AK155, by transformation of T lymphocytes with herpesvirus saimiri. J Virol. 2000; 74:3881–3887. [PubMed: 10729163]
53. Wilson NJ, Boniface K, Chan JR, McKenzie BS, Blumenschein WM, Mattson JD, Basham B, Smith K, Chen T, Morel F, et al. Development, cytokine profile and function of human interleukin 17-producing helper T cells. Nat Immunol. 2007; 8:950–957. [PubMed: 17676044]
54. Corvaisier M, Delneste Y, Jeanvoine H, Preisser L, Blanchard S, Garo E, Hoppe E, Barré B, Audran M, Bouvard B, et al. IL-26 is overexpressed in rheumatoid arthritis and induces proinflammatory cytokine production and Th17 cell generation. PLoS Biol. 2012; 10:e1001395. [PubMed: 23055831]
55. Goris A, Marrosuand MG, Vandenbroeck K. Novel polymorphisms in the IL-10 related AK155 gene (chromosome 12q15). Genes Immun. 2001; 2:284–286. [PubMed: 11528524]
56. Vandenbroeck K, Cunningham S, Goris A, Alloza I, Heggarty S, Graham C, Bell A, Rooney M. Polymorphisms in the interferon-gamma/interleukin-26 gene region contribute to sex bias in susceptibility to rheumatoid arthritis. Arthritis Rheum. 2003; 48:2773–2778. [PubMed: 14558082]
57. Silverberg MS, Cho JH, Rioux JD, McGovern DP, Wu J, Annese V, Achkar JP, Goyette P, Scott R, Xu W, et al. Ulcerative colitis-risk loci on chromosomes 1p36 and 12q15 found by genome-wide association study. Nat Genet. 2009; 41:216–220. [PubMed: 19122664]

Author Manuscript Author Manuscript Author Manuscript Author Manuscript

58. Miot C, Beaumont E, Duluc D, Le Guillou-Guillemette H, Preisser L, Garo E, Blanchard S, HubertFouchard I, Créminon C, Lamourette P, et al. IL-26 is overexpressed in chronically HCV-infected patients and enhances TRAIL-mediated cytotoxicity and interferon production by human NK cells. Gut. 201410.1136/gutjnl-2013-306604

59. Wolk K, Kunz S, Asadullah K, Sabat R. Cutting edge: immune cells as sources and targets of the IL-10 family members? J Immunol. 2002; 168:5397–5402. [PubMed: 12023331]

60. Carlson MJ, West ML, Coghill JM, Panoskaltsis-Mortari A, Blazar BR, Serody JS. In vitro-differentiated TH17 cells mediate lethal acute graft-versus-host disease with severe cutaneous and pulmonary pathologic manifestations. Blood. 2009; 113:1365–1374. [PubMed: 18957685]

61. Fan L, Benson HL, Vittal R, Mickler EA, Presson R, Fisher AJ, Cummings OW, Heidler KM, Keller MR, Burlinghamand WJ, Wilkes DS. Neutralizing IL-17 prevents obliterative bronchiolitis in murine orthotopic lung transplantation. Am J Transplant. 2011; 11:911–922. [PubMed: 21521466]

62. Burlingham WJ, Love RB, Jankowska-Gan E, Haynes LD, Xu Q, Bobadilla JL, Meyer KC, Hayney MS, Braun RK, Greenspan DS, et al. IL-17-dependent cellular immunity to collagen type V predisposes to obliterative bronchiolitis in human lung transplants. J Clin Invest. 2007; 117:3498–3506. [PubMed: 17965778]

63. Serody JS, Hill GR. The IL-17 differentiation pathway and its role in transplant outcome. Biol Blood Marrow Transplant. 2012; 18:S56–S61. [PubMed: 22226114]

64. Muranski P, Restifo NP. Essentials of Th17 cell commitment and plasticity. Blood. 2013; 121:2402–2414. [PubMed: 23325835]

65. Flynn R, Du J, Veenstra RG, Reichenbach DK, Panoskaltsis-Mortari A, Taylor PA, Freeman GJ, Serody JS, Murphy WJ, Munn DH, et al. Increased T follicular helper cells and germinal center B cells are required for cGVHD and bronchiolitis obliterans. Blood. 2014; 123:3988–3998. [PubMed: 24820310]

66. Zhang C, Todorov I, Zhang Z, Liu Y, Kandeel F, Forman S, Strober S, Zeng D. Donor $CD4^+$ T and B cells in transplants induce chronic graft-versus-host disease with autoimmune manifestations. Blood. 2006; 107:2993–3001. [PubMed: 16352808]

67. Ishikawa F, Yasukawa M, Lyons B, Yoshida S, Miyamoto T, Yoshimoto G, Watanabe T, Akashi K, Shultz LD, Harada M. Development of functional human blood and immune systems in NOD/SCID/IL2 receptor γ $chain^{null}$ mice. Blood. 2005; 106:1565–1573. [PubMed: 15920010]

68. Schwab L, Goroncy L, Palaniyandi S, Gautam S, Triantafyllopoulou A, Mocsai A, Reichardt W, Karlsson FJ, Radhakrishnan SV, Hanke K, et al. Neutrophil granulocytes recruited upon translocation of intestinal bacteria enhance graft-versus-host disease via tissue damage. Nat Med. 2014; 20:648–654. [PubMed: 24836575]

69. Campbell TB, Hangoc G, Liu Y, Pollokand K, Broxmeyer HE. Inhibition of CD26 in human cord blood $CD34^+$ cells enhances their engraftment of nonobese diabetic/severe combined immunodeficiency mice. Stem Cells Dev. 2007; 16:347–354. [PubMed: 17610364]

70. Christopherson KW II, Hangoc G, Manteland CR, Broxmeyer HE. Modulation of hematopoietic stem cell homing and engraftment by CD26. Science. 2004; 305:1000–1003. [PubMed: 15310902]

71. Broxmeyer HE, Hoggatt J, O'Leary HA, Mantel C, Chitteti BR, Cooper S, Messina-Graham S, Hangoc G, Farag S, Rohrabaugh SL, et al. Dipeptidylpeptidase 4 negatively regulates colony-stimulating factor activity and stress hematopoiesis. Nat Med. 2012; 18:1786–1796. [PubMed: 23160239]

72. Farag SS, Srivastava S, Messina-Graham S, Schwartz J, Robertson MJ, Abonour R, Cornetta K, Wood L, Secrest A, Strother RM, et al. In vivo DPP-4 inhibition to enhance engraftment of single-unit cord blood transplants in adults with hematological malignancies. Stem Cells Dev. 2013; 22:1007–1015. [PubMed: 23270493]

73. Ohnuma K, Inoue H, Uchiyama M, Yamochi T, Hosono O, Dangand NH, Morimoto C. T-cell activation via CD26 and caveolin-1 in rheumatoid synovium. Mod Rheumatol. 2006; 16:3–13. [PubMed: 16622717]

74. Blazar BR, Taylor PA, Boyer MW, Panoskaltsis-Mortari A, Allison JP, Vallera DA. CD28/B7 interactions are required for sustaining the graft-versus-leukemia effect of delayed post-bone

Author Manuscript Author Manuscript Author Manuscript Author Manuscript

marrow transplantation splenocyte infusion in murine recipients of myeloid or lymphoid leukemia cells. J Immunol. 1997; 159:3460–3473. [PubMed: 9317145]

75. Hatano R, Yamada T, Matsuoka S, Iwata S, Yamazaki H, Komiya E, Okamoto T, Dang NH, Ohnuma K, Morimoto C. Establishment of monoclonal anti-human CD26 antibodies suitable for immunostaining of formalin-fixed tissue. Diagn Pathol. 2014; 9:30–42. [PubMed: 24502396]

Author Manuscript Author Manuscript Author Manuscript Author Manuscript

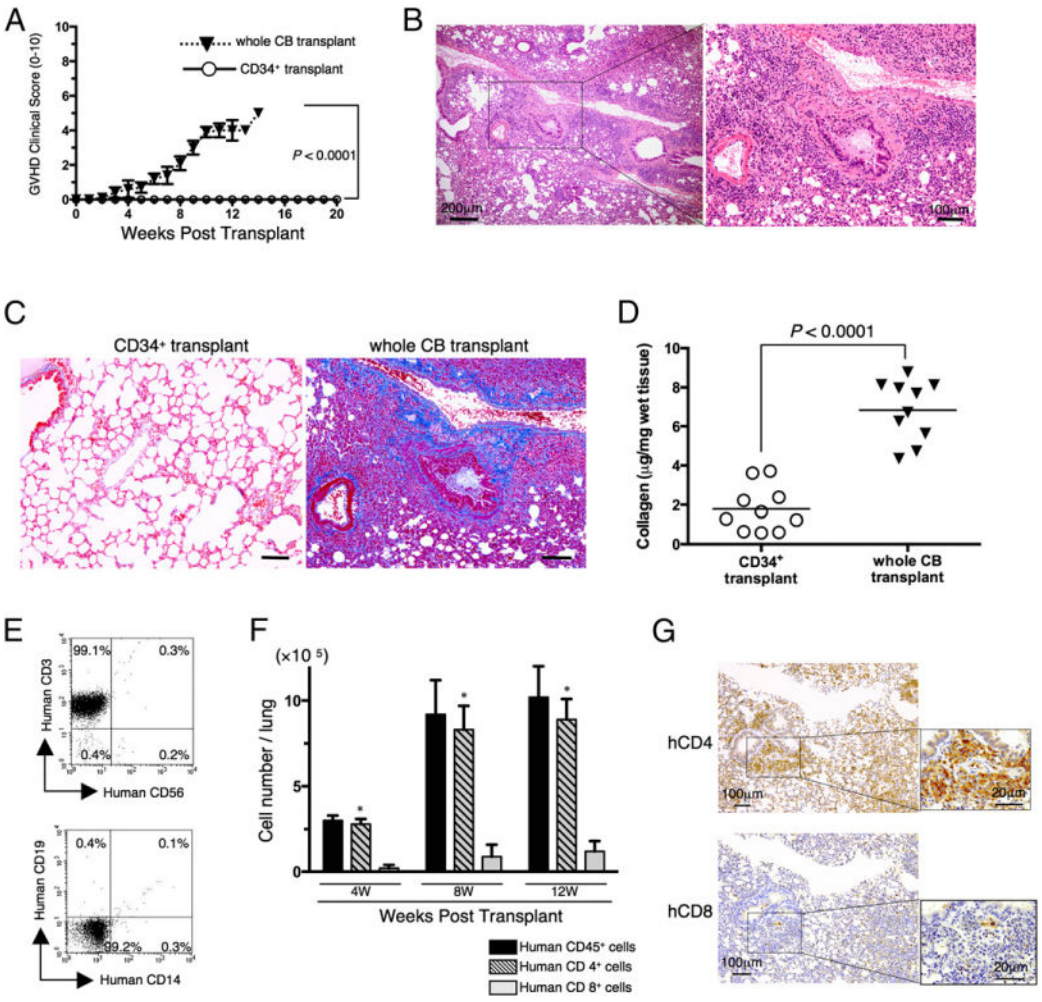

FIGURE 1.

Obliterative bronchiolitis in sublethally irradiated NOG mice transplanted with HuCB cells. NOG mice were irradiated at sublethal dose (200 cGy) and the next day were transplanted with 1×10^5 T cell–depleted $CD34^+$ cells purified from HuCB ($CD34^+$ transplant) or with 1×10^7 MNCs isolated from HuCB (whole CB transplant). (**A**) Clinical GVHD score (mean ± SEM). Data are cumulative results from three independent experiments (for each, $n = 10$). The p value was calculated by log-rank test. (**B**) H&E staining of the lung of whole CB transplant (8 wk posttransplantation). The *left panel* shows lower original magnification (×40) and the *right panel* shows higher original magnification (×100). Representative histology is shown from three independent experiments (for each, $n = 10$). (**C**) Collagen deposition was evaluated in the lung tissues of $CD34^+$ or whole CB transplant (8 wk posttransplantation) with an Azan-Mallory staining. The histology shown in whole CB transplant is a sequential section of (B). Dark blue areas indicating collagen deposition are clearly observed in whole CB transplant mice, compared with those in $CD34^+$ transplant mice. Representative histology is shown from three independent experiments (for each, $n = 10$). Original magnification ×100. Scale bars, 100 μm. (**D**) Collagen contents in the lung were quantified by Sircol Collagen Assay. The mean number (±SEM) of total collagen contents (μg) per wet lung tissue weight (mg) was determined from three independent

Author Manuscript Author Manuscript Author Manuscript Author Manuscript

experiments (for each, $n = 10$). Increased collagen contents were clearly observed in whole CB transplant mice, compared with those in $CD34^+$ transplant mice. Each dot indicates individual value, and horizontal bars indicate mean value. (**E**) Representative two-dimensional dot plots of human lymphocyte composition in the lung of whole CB transplant mice (8 wk posttransplantation). Single-suspension cells isolated from the lung of whole CB transplant mice (8 wk posttransplantation) were sorted by human $CD45^+$ cells and then analyzed using flow cytometry. The *upper panel* shows representative human CD3 and/or CD56 staining, and the *lower panel* shows representative human CD19 and/or CD14 staining. Numbers indicate relative percentages per quadrant. Similar results were observed in independent experiments ($n = 8$). (**F**) Absolute cell numbers (mean ± SEM) of human $CD45^+$, $CD4^+$, or $CD8^+$ cells per lung of whole CB transplant mice were quantified by flow cytometry. $CD4^+$ T cells were predominantly observed in the lung of whole CB transplant mice. Data are cumulative results from three independent experiments ($n = 10$ at 4 wk, $n = 8$ at 8 wk, and $n = 3$ at 12 wk). $^*p < 0.0001$ versus $CD8^+$ cells. (**G**) Anti-human CD4 or CD8 immunohistochemistry of sequential sections of lung tissue of whole CB transplant mice (8 wk posttransplantation). Predominant infiltration of $CD4^+$ cells was observed, with similar results to those obtained by flow cytrometry, as shown in (F). Representative histology is shown from three independent experiments (for each, $n = 10$). Original magnification ×100 or ×400 (*inset* in each panel).

Author Manuscript Author Manuscript Author Manuscript Author Manuscript

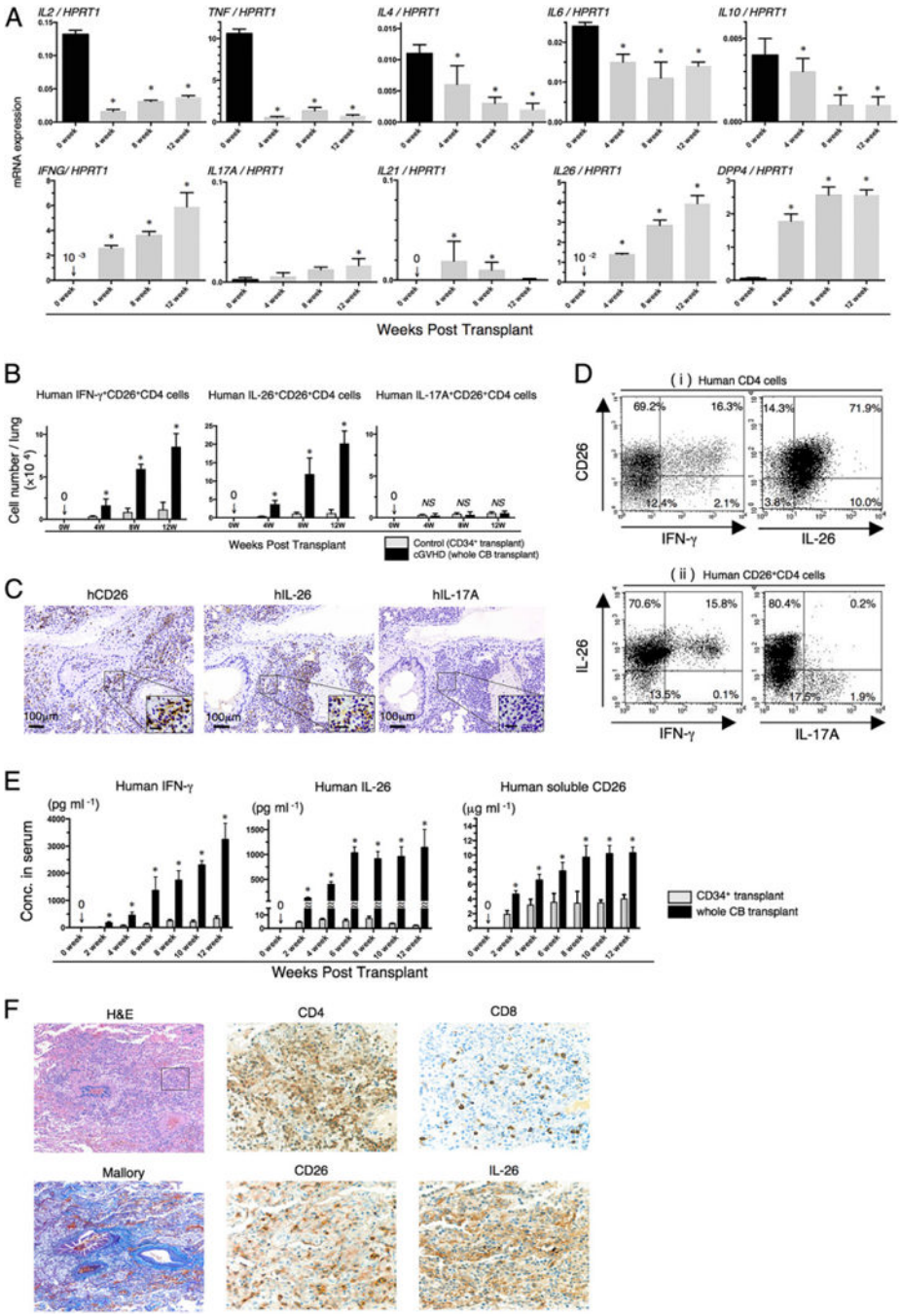

FIGURE 2.

Predominant infiltration of IL-26$^+$CD26$^+$CD4 T cells in the lung of obliterative bronchiolitis. (**A**) Whole CB transplant mice were sacrificed at 4, 8, and 12 wk posttransplantation, and the lungs were removed, followed by isolation of human CD4$^+$ cells. mRNA expression of human cytokines or CD26/DPP4 was quantified by real-time RT-PCR. Each expression was normalized to HPRT1. Data at 0 wk were obtained using freshly isolated HuCB CD4 T cells of three different donors. Data are cumulative results from three independent experiments (n = 10 at 4 wk, n = 8 at 8 wk, and n = 3 at 12 wk). *p <

Author Manuscript Author Manuscript Author Manuscript Author Manuscript

0.0001 versus each at 0 wk. (**B**) Absolute cell numbers of human IFN-γ^+CD26$^+$CD4, IL-26$^+$CD26$^+$CD4, or IL-17A$^+$CD26$^+$CD4 cells in the lung of CD34$^+$ transplant or whole CB transplant mice were quantified by flow cytometry. Data are cumulative results from three independent experiments (for each, $n = 10$ in CD34$^+$ transplant group, and $n = 10$ at 4 wk, $n = 8$ at 8 wk, and $n = 3$ at 12 wk in whole CB transplant group). *$p < 0.0001$ versus corresponding CD34$^+$ transplant group. (**C**) Anti-human CD26, IL-26, or IL-17A immunohistochemical staining of sequential sections of the lung from whole CB transplant mice (8 wk posttransplantation). The lung of whole CB transplant mice was clearly infiltrated with human CD26 or IL-26 (brown stained cells), but not with IL-17A–positive cells. Representative histology is shown from three independent experiments ($n = 10$). Original magnification ×100 or ×400 (*inset* in each panel). Scale bars in the *inset*, 20 μm. (**D**) Representative two-dimensional dot plots of human CD26 and IFN-γ or IL-26 cells by gating for human CD4$^+$ cells (D**i**), and of human IFN-γ or IL-17A among IL-26$^+$ cells by gating for human CD26$^+$CD4$^+$ cells (D**ii**). Single-suspension cells isolated from the lung of whole CB transplant mice (8 wk posttransplantation) were sorted by human CD45$^+$ cells and then analyzed using flow cytometry. Numbers indicate relative percentages per quadrant. Similar results were observed in independent experiments ($n = 10$). (**E**) Sera of CD34$^+$ transplant or whole CB transplant mice were collected at the indicated week posttransplantation, and serum levels of human IFN-γ, IL-26, and soluble CD26/DPP4 were quantified. Data are cumulative results from three independent experiments (for each, $n = 10$ in CD34$^+$ transplant group, and $n = 10$ at 0–6 wk, $n = 8$ at 8 wk, $n = 7$ at 10 wk, and $n = 3$ at 12 wk in whole CB transplant group). *$p < 0.0001$ versus corresponding CD34$^+$ transplant group. (**F**) H&E, Azan-Mallory, anti-human CD4, CD8, CD26, or IL-26 immunohistochemical staining of sequential sections of the lung from a patient undergoing alloPBSCT for ALL. After having acute skin GVHD on day +33 posttransplant, the patient experienced dyspnea with ground glass opacity detected on the chest X-ray examination on day +95. The lung specimen was obtained by transbronchial lung biopsy on day +101, showing perivascular and subepithelial inflammation and narrowing of the bronchiole (H&E staining). Peribronchiolar and perivascular collagen deposition was detected by Azan-Mallory staining. The lung was clearly infiltrated with CD4-, CD26-, or IL-26–positive cells (brown stained cells), with CD8-positive cells found at a very low level. The histology shown in immunohistochemical staining is focused in the *inset* of the H&E staining panel. Original magnification ×100 (H&E and Azan-Mallory) or ×400 (anti-CD4, CD8, CD26, and IL-26 staining).

Author Manuscript
Author Manuscript
Author Manuscript
Author Manuscript

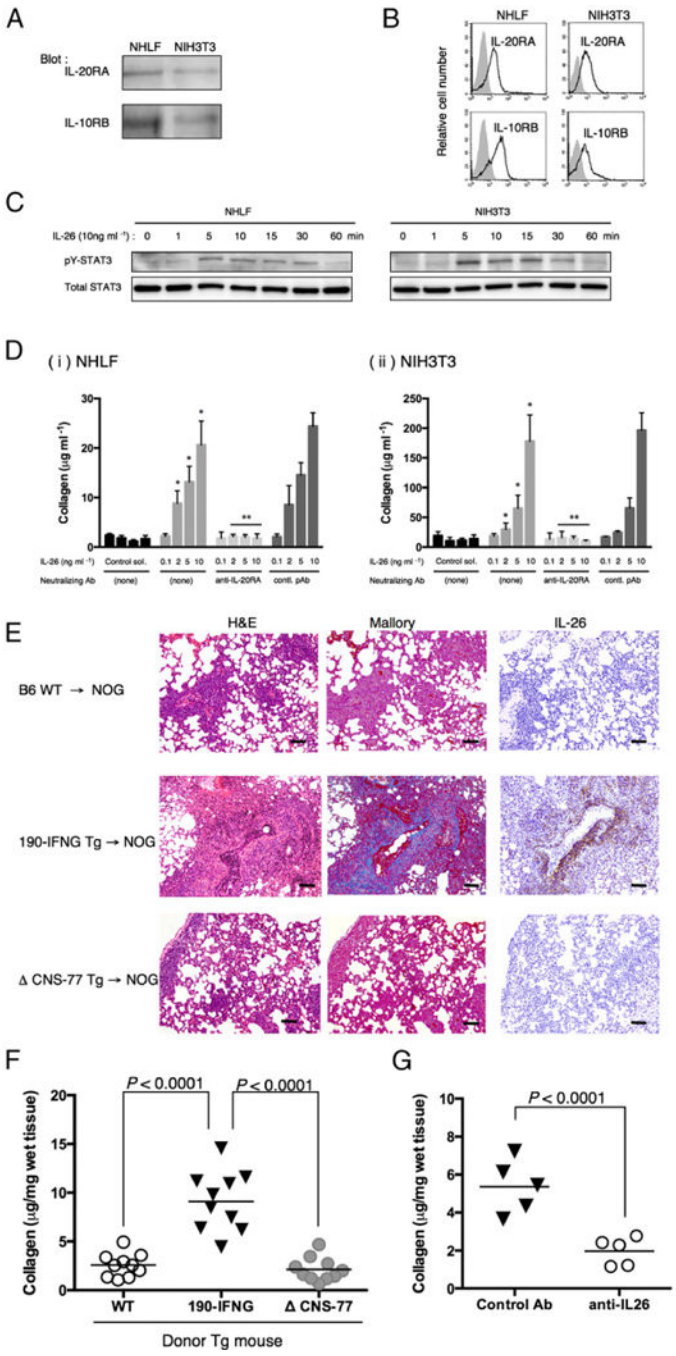

FIGURE 3.

IL-26 stimulates fibroblast, and collagen deposition in the lung of obliterative bronchiolitis is induced in NOG mice receiving bone marrow cells and splenocytes of *IL26* Tg mice. (**A**) Western blot analysis of IL-20RA and IL-10RB in NHLF and NIH3T3 cells. Lysates (each, 10 μg) were prepared using RIPA buffer, being resolved by SDS-PAGE in reducing condition and immunoblotted using anti–IL-20RA or anti–IL-10RB pAbs recognizing both human and murine Ags. (**B**) Representative histogram of IL-20RA and IL-10RB of NHLF and NIH3T3 cells. Single-suspension cells were stained with anti–IL-20RA or anti–IL-10RB

Author Manuscript Author Manuscript Author Manuscript Author Manuscript

pAbs recognizing both human and murine Ags, and analyzed using flow cytometry (bold line). Gray histograms indicate isotype control (rabbit polyclonal IgG and anti-rabbit IgG-PE). (**C**) A total of 1×10^5 cells of NHLF or NIH3T3 was seeded in 96-well flat-bottom plate, and the next day IL-26 (10 ng ml^{-1} in PBS) was added to each well. Cells were harvested at each time point, and cell lysates were prepared in RIPA buffer containing Halt Protease and Phosphatase inhibitor mixture, and 10 μg each lysate was resolved by SDS-PAGE in reducing condition and immunoblotted with antiphosphorylated STAT3 (pY-STAT3) recognizing both human and murine Ags, followed by stripping and reprobing with anti-STAT3 pAb (total STAT3) recognizing both human and murine Ags. Representative data are shown from three independent experiments with similar results. (**D**) Collagen production of NHLF (D**i**) or NIH3T3 (D**ii**) cells stimulated with exogenous IL-26 in the presence or absence of neutralizing anti–IL-20RA pAb or rabbit Ig (contl. pAb). Data are shown as mean ± SEM, resulting from three independent experiments with triplicates. The amount of secreted soluble collagen increased with increasing level of exogenous IL-26 in a dose-dependent manner (*$p < 0.0001$ versus corresponding control solvent), and production of collagen was inhibited by the presence of neutralizing anti–IL-20RA pAb (**$p < 0.0001$ versus corresponding contl. pAb). (**E**) H&E, Azan-Mallory staining, and anti–IL-26 immunohistochemical staining of sequential sections of the lung from NOG mice at 4 wk after transplantation of BM and splenocytes isolated from parental B6 (B6 WT), 190-*IFNG* BAC Tg (190-IFNG Tg), or ΔCNS-77 Tg mice. The lung of recipients of 190-IFNG Tg mice showed obliterative bronchiolitis with collagen deposition and IL-26^+ cell infiltration, whereas recipients of B6 WT or ΔCNS-77 Tg mice showed peribronchial and septal infiltration without collagen deposition or IL-26^+ cells. Representative histology is shown from three independent experiments (for each, $n = 6$). Original magnification ×100. Scale bars, 100 μm. (**F**) Recipient mice were sacrificed at 4 wk posttransplantation, and the lungs were removed. Collagen contents in the lung were quantified by Sircol Collagen Assay. The mean number (±SEM) of total collagen contents (μg) per wet lung tissue weight (mg) was determined from three independent experiments (for each, $n = 10$). Increased collagen contents were clearly observed in recipients of 190-IFNG Tg mice, compared with those in recipients of B6 WT or ΔCNS-77 Tg mice. Each dot indicates individual value, and horizontal bars indicate mean value. (**G**) Whole CB transplant mice were administered anti–IL-26 Ab or control Ab (each 50 μg/dose) i.p. thrice per week, beginning at day +21 after transplantation until day +32. Recipient mice were sacrificed at 5 wk posttransplantation, and the lungs were removed. Collagen contents in the lung were quantified by Sircol Collagen Assay. The mean number (±SEM) of total collagen contents (μg) per wet lung tissue weight (mg) was determined from two independent experiments (for each, $n = 5$). Decreased collagen contents were clearly observed in the recipients of anti–IL-26 Ab. Each dot indicates individual value, and horizontal bars indicate mean value.

Author Manuscript Author Manuscript Author Manuscript Author Manuscript

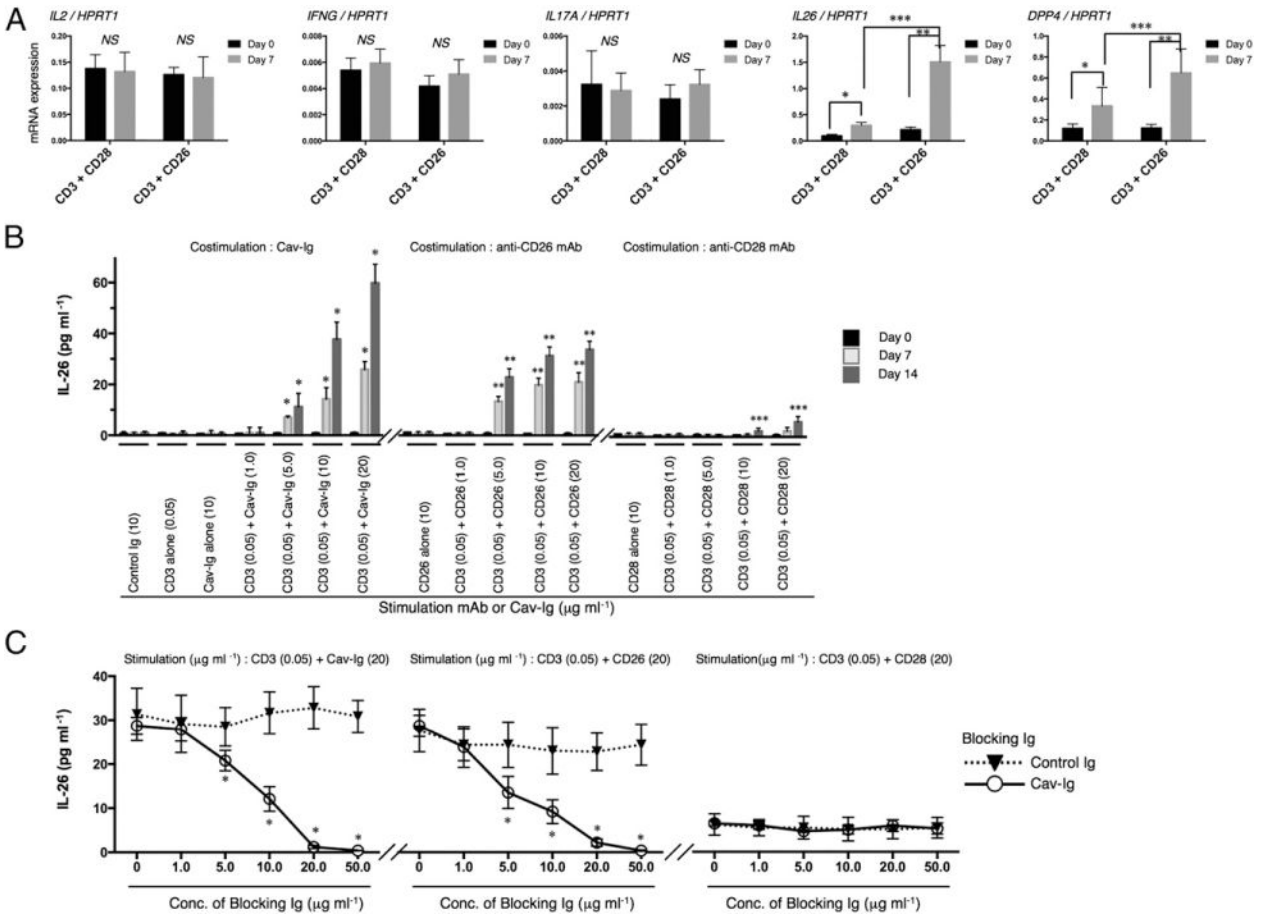

FIGURE 4.

CD26 costimulation enhances IL-26 production in HuCB CD4 T cells, and blockade by the CD26 ligand caveolin-1 reduces production of IL-26. (**A**) HuCB CD4 T cells were stimulated with immobilized anti-CD3 (0.05 μg ml^{-1}) plus anti-CD28 (10 μg ml^{-1}) or anti-CD26 (10 μg ml^{-1}) mAbs. After 7 d of stimulation, mRNA levels of human *IL2*, *IFNG*, *IL17A*, *IL26*, and *DPP4* were quantified by real-time RT-PCR. Each expression was normalized to HPRT1. Data are shown as mean ± SEM, resulting from three independent experiments with triplicates. *$p < 0.05$, **,***$p < 0.0001$. (**B**) HuCB CD4 T cells were stimulated with plate-bound anti-CD3, anti-CD28, anti-CD26 mAbs, or Cav-Ig immobilized at the indicated concentration. The supernatants were harvested 7 or 14 d after stimulation, and levels of human IL-26 were quantified. Data are shown as mean ± SEM, resulting from three independent experiments with triplicates (*,**$p < 0.0001$ or ***$p < 0.05$ versus corresponding samples at day 0). (**C**) HuCB CD4 T cells were treated with blocking Cav-Ig (solid line) or control Ig (dotted line) at the indicated concentration. After 1 h of incubation with blocking Cav-Ig or control Ig, cells were stimulated with immobilized anti-CD3 (0.05 μg ml^{-1}) plus Cav-Ig (20 μg ml^{-1}), anti-CD28 (20 μg ml^{-1}), or anti-CD26 (20 μg ml^{-1}) mAbs. After 7 d of stimulation, the supernatants were harvested and levels of human IL-26 were quantified. Data are shown as mean ± SEM, resulting from three independent experiments with triplicates. *$p < 0.0001$ versus corresponding control Ig.

Author Manuscript Author Manuscript Author Manuscript Author Manuscript

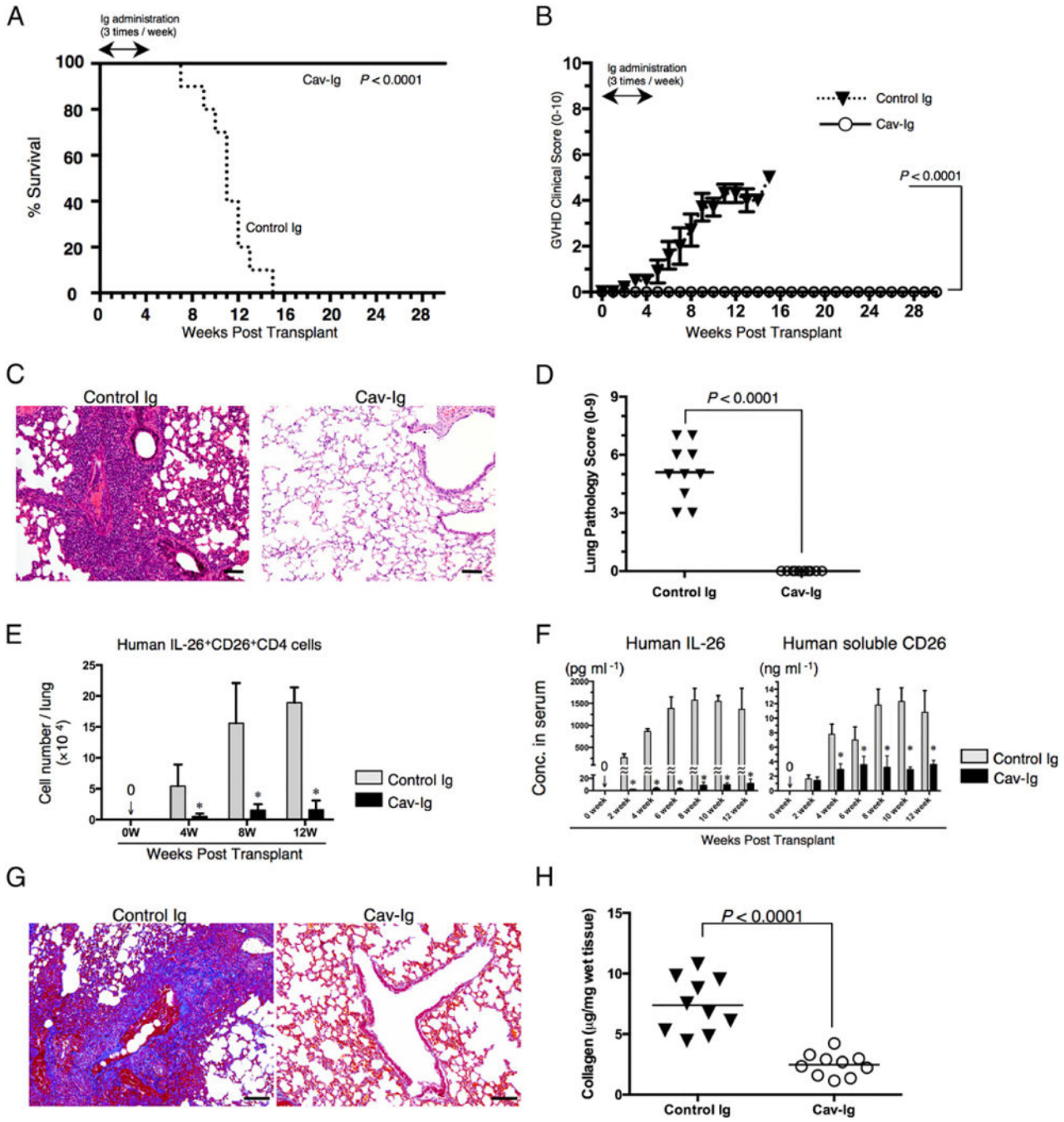

FIGURE 5.

Administration of Cav-Ig prevents obliterative bronchiolitis by reducing level of IL-26^{+}CD26^{+}CD4 cells and collagen deposition. Sublethally irradiated NOG mice were transplanted with 1×10^{7} MNCs isolated from HuCB. Cav-Ig or control Ig (each 100 μg/dose) was administered i.p. thrice per week, beginning at day +1 after transplantation until day +28. (**A**) Overall survival and (**B**) clinical GVHD score (mean ± SEM). Data are cumulative results from three independent experiments (for each, $n = 10$). (**C**) H&E staining of the lung of recipients administered with control Ig or Cav-Ig group (6 wk

Author Manuscript Author Manuscript Author Manuscript Author Manuscript

posttransplantation). Representative histology is shown from three independent experiments (for each, $n = 10$). Original magnification ×100. Scale bars, 100 μm. (**D**) Pathologic damage in the lung of recipients administered with Cav-Ig or control Ig was examined at 6 wk posttransplantation, using a semiquantitative scoring system. Each dot indicates individual value, and horizontal bars indicate mean value. (**E**) Absolute cell number of human IL-26$^+$CD26$^+$CD4 cells in the lung of recipients of Cav-Ig or control Ig group. Data are cumulative results from three independent experiments (for each, $n = 10$ in Cav-Ig group, and $n = 10$ at 0–4 wk, $n = 9$ at 8 wk, and $n = 2$ at 12 wk in control Ig group). *$p < 0.0001$ versus corresponding control Ig group. (**F**) Sera of recipients of Cav-Ig or control Ig group were collected at the indicated week posttransplantation, and serum levels of human IL-26 and soluble CD26/DPP4 were quantified. Data are cumulative results from three independent experiments (for each, $n = 10$ in Cav-Ig group, and $n = 10$ at 0–6 wk, $n = 9$ at 8 wk, $n = 7$ at 10 wk, and $n = 2$ at 12 wk in control Ig group). *$p < 0.0001$ versus corresponding control Ig group. (**G**) Collagen deposition was determined in the lung tissues of recipients of Cav-Ig or control Ig group (6 wk posttransplantation) with an Azan-Mallory staining. Representative histology is shown from three independent experiments (for each, $n = 6$). Original magnification ×100. Scale bars, 100 μm. (**H**) Collagen contents in the lung of recipients of Cav-Ig or control Ig group (6 wk posttransplantation) were quantified by Sircol Collagen Assay. The mean number (±SEM) of total collagen contents (μg) per wet lung tissue weight (mg) was determined from three independent experiments (for each, $n = 10$). Decreased collagen contents were clearly observed in recipients of Cav-Ig group. Each dot indicates individual value, and horizontal bars indicate mean value.

Author Manuscript
Author Manuscript
Author Manuscript
Author Manuscript

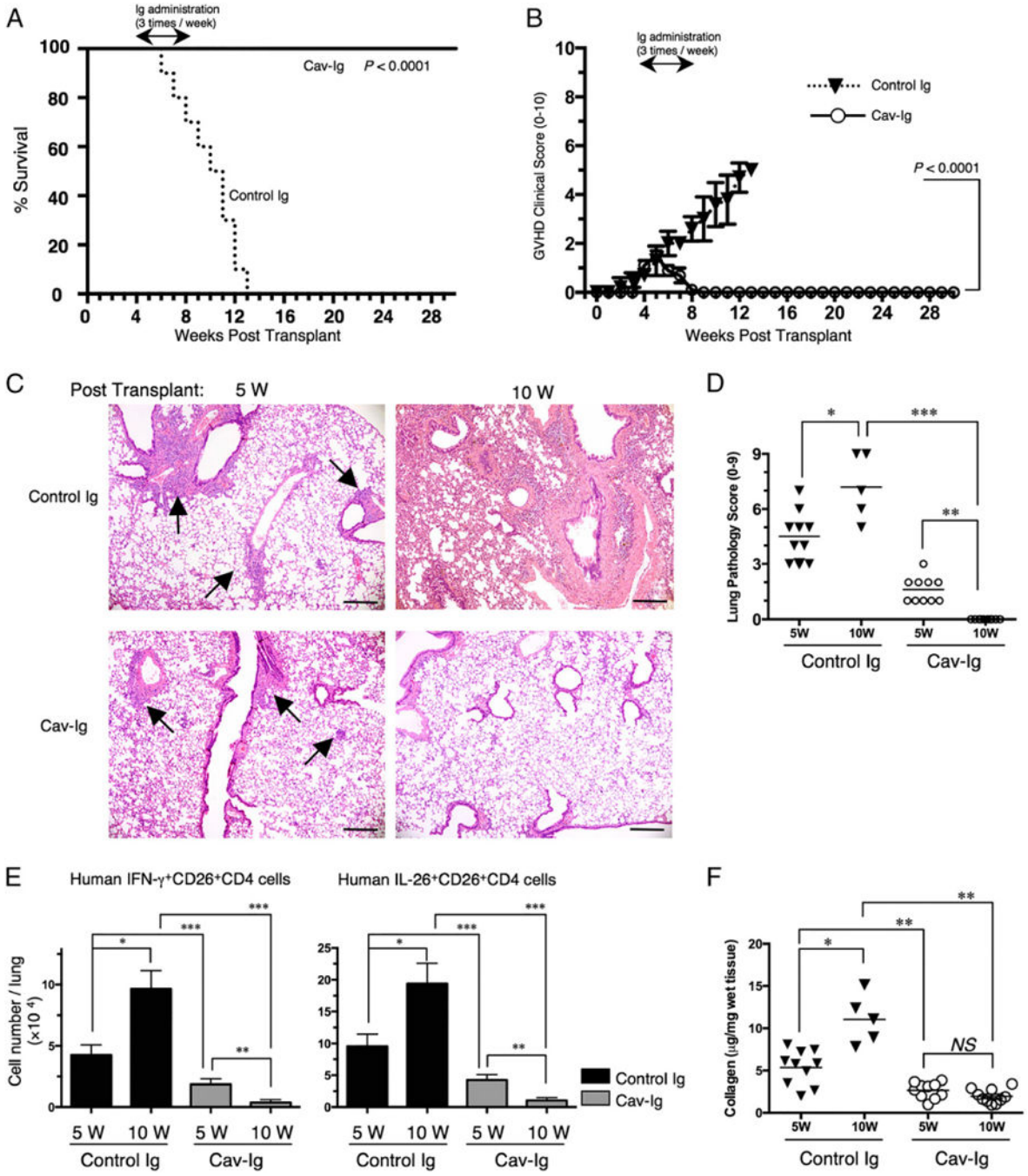

FIGURE 6.

Administration of Cav-Ig during early GVHD development impedes lethal GVHD by reducing level of IL-26^{+}CD26^{+}CD4 cells and collagen deposition in the lung. Sublethally irradiated NOG mice were transplanted with 1 × 10^{7} MNCs isolated from HuCB. Cav-Ig or control Ig (each 100 mg/dose) was administered i.p. thrice per week, beginning at day +29 after transplantation until day +56. (**A**) Overall survival and (**B**) clinical GVHD score (mean ± SEM). Data are cumulative results from three independent experiments (for each, n = 10). (**C**) H&E staining of the lung tissues of control Ig group and Cav-Ig group at 5 or 10 wk

Author Manuscript Author Manuscript Author Manuscript Author Manuscript

posttransplantation. Representative histology is shown from three independent experiments (for each, $n = 10$ in Cav-Ig group, and $n = 10$ at 5 wk and $n = 5$ at 10 wk in control Ig group). Arrows indicate perivascular and peribronchial inflammation of the small airway. Original magnification ×100. Scale bars, 100 μm. (**D**) Pathologic damage in the lung of recipients administered with Cav-Ig or control Ig was examined at 5 and 10 wk posttransplantation using a semiquantitative scoring system. Each dot indicates individual value, and horizontal bars indicate mean value. Data are cumulative results from three independent experiments (for each, $n = 10$ in Cav-Ig group, and $n = 10$ at 5 wk and $n = 5$ at 10 wk in control Ig group). $*p < 0.01$, $**,***p < 0.0001$. (**E**) Absolute cell number of human IFN-γ^+ or IL-26^+CD26^+CD4 cells in the lung of recipients of Cav-Ig or control Ig group. Data are cumulative results from three independent experiments (for each, $n = 10$ in Cav-Ig group, and $n = 10$ at 5 wk and $n = 5$ at 10 wk in control Ig group). $*,**,***p < 0.0001$. (**F**) Collagen contents in the lung of recipients of Cav-Ig or control Ig group (5 and 10 wk posttransplantation) were quantified by Sircol Collagen Assay. The mean number (±SEM) of total collagen contents (μg) per wet lung tissue weight (mg) was determined from three independent experiments (for each, $n = 10$ in Cav-Ig group, and $n = 10$ at 5 wk and $n = 5$ at 10 wk in control Ig group). Each dot indicates individual value, and horizontal bars indicate mean value. $*,**p < 0.0001$.

Author Manuscript Author Manuscript Author Manuscript Author Manuscript

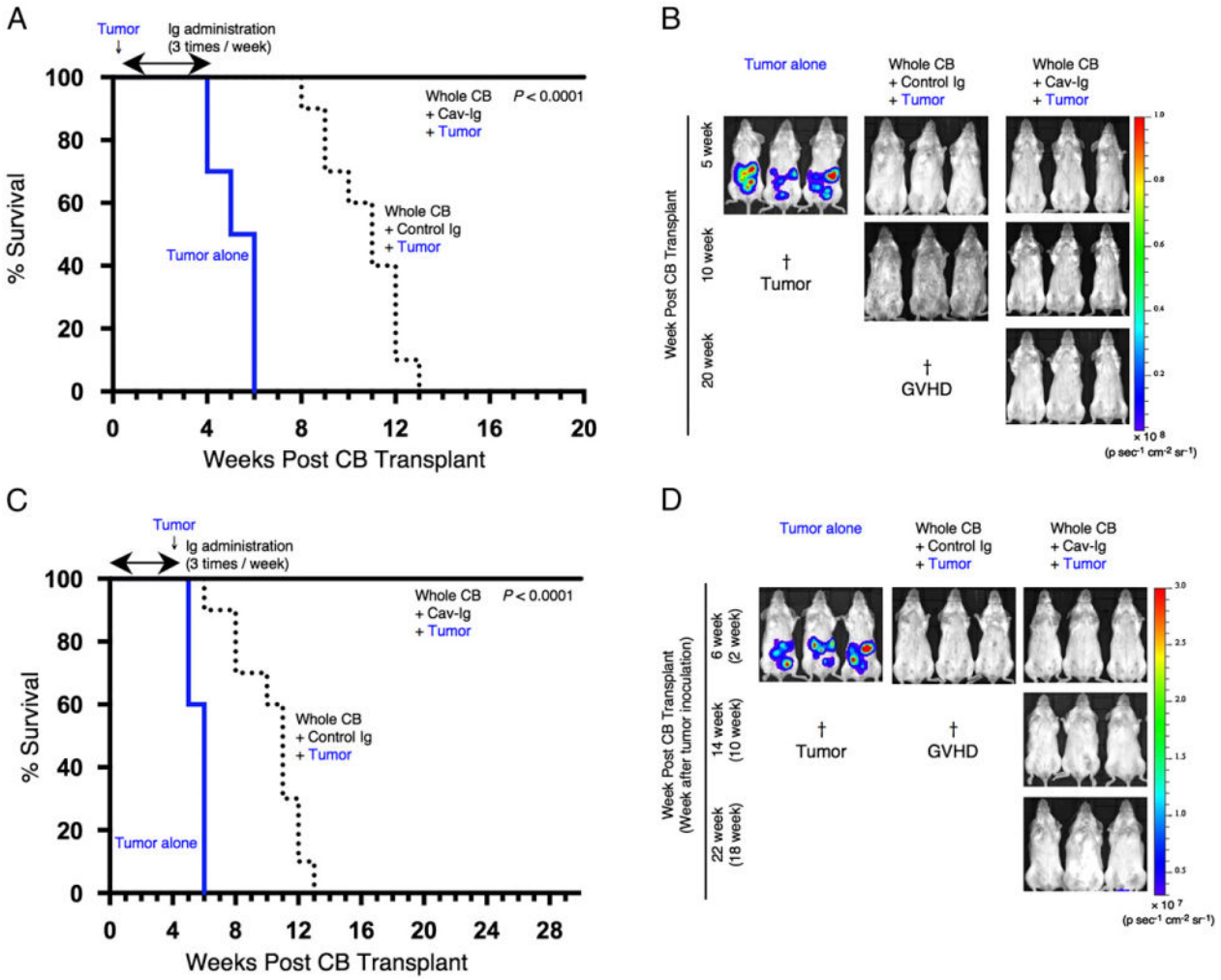

FIGURE 7.

Cav-Ig preserves GVL effect. (**A**) NOG mice were irradiated at sublethal dose (200 cGy) and the next day were inoculated with 1×10^4 A20-luc cells via tail vein, and then were transplanted the following day with 1×10^7 MNCs isolated from HuCB. Cav-Ig or control Ig (each 100 μg/dose) was administered i.p. thrice per week, beginning at day +1 after transplantation until day +28. Overall survival is depicted from cumulative results from three independent experiments (for each, $n = 10$). $p < 0.0001$ versus recipients of control Ig by log-rank test. (**B**) In vivo bioluminescence imaging was performed at the indicated time points after treatment, as described in (A). Representative mice are shown. Ruffled fur consistent with skin GVHD is shown in recipients of control Ig group at 10 wk posttransplant (*middle panel*). †Death of all mice in the group of tumor alone or control Ig groups. (**C**) Sublethally irradiated NOG mice were transplanted with MNCs isolated from HuCB. Cav-Ig or control Ig was administered i.p. thrice per week, beginning at day +1 after transplantation until day +28. A total of 1×10^5 A20-luc cells was inoculated via tail vein on day +28 posttransplantation. Overall survival is depicted from cumulative results from three independent experiments (for each, $n = 10$). $p < 0.0001$ versus recipients of control Ig by log-rank test. (**D**) In vivo bioluminescence imaging was performed at the indicated time

points after treatment, as described in (C). Representative mice are shown. Slightly ruffled fur consistent with skin GVHD is shown in recipients of control Ig group at 6 wk posttransplant (*middle panel*). †Death of all mice in the group of tumor alone or control Ig groups.

Author Manuscript Author Manuscript Author Manuscript Author Manuscript